ANALYSIS OF LINEAR ANTENNA SYSTEMS: A DIFFERENT APPROACH

SATISH KUMAR SRIVASTAVA


CENTRE FOR NFLD. STUDIES
JUL 18 1978
MEMORIAL UNIVERSITY
OF NEWFOUNDLAND

NOTICE

The quality of this microfiche is heavily dependent upon the quality of the original thesis submitted for microfilming. Every effort has been made to ensure the highest quality of reproduction possible.

If pages are missing, contact the university which granted the degree.

Some pages may have indistinct print especially if the original pages were typed with a poor typewriter ribbon or if the university sent us a poor photocopy.

Previously copyrighted materials (journal articles, published tests, etc.) are not filmed.

Reproduction in full or in part of this film is governed by the Canadian Copyright Act, R.S.C. 1970, c. C-30. Please read the authorization forms which accompany this thesis.

THIS DISSERTATION
HAS BEEN MICROFILMED
EXACTLY AS RECEIVED

AVIS

La qualité de cette microfiche dépend grandement de la qualité de la thèse soumise au microfilmage. Nous avons tout fait pour assurer une qualité supérieure de reproduction.

S'il manque des pages, veuillez communiquer avec l'université qui a conféré le grade.

La qualité d'impression de certaines pages peut laisser à désirer, surtout si les pages originales ont été dactylographiées à l'aide d'un ruban usé ou si l'université nous a fait parvenir une photocopie de mauvaise qualité.

Les documents qui font déjà l'objet d'un droit d'auteur (articles de revue, examens publiés, etc.) ne sont pas microfilmés.

La reproduction, même partielle, de ce microfilm est soumise à la Loi canadienne sur le droit d'auteur, SRC 1970, c. C-30. Veuillez prendre connaissance des formules d'autorisation qui accompagnent cette thèse.

LA THÈSE A ÉTÉ
MICROFILMÉE TELLE QUE
NOUS L'AVONS REÇUE

ANALYSIS OF LINEAR ANTENNA SYSTEMS: A DIFFERENT APPROACH

by

Satish Kumar Srivastava, B.Sc.Eng. (Hons.)

A Thesis submitted in partial fulfillment
of the requirements for the degree of
Master of Engineering

Faculty of Engineering and Applied Science
Memorial University of Newfoundland

July 1977

St. John's Newfoundland

ABSTRACT

A method of analysis of linear antenna systems for finding the current distributions subjected to a known incident electrical field is proposed. This method is an application of a proposed general procedure for the solution of antenna and scattering problems. The practice of solving an integral equation directly for the unknown current distribution is replaced by that of solving an integral equation for an unknown intermediate function. This intermediate function is shown to be the forcing function of a differential equation whose closed form solution yields the unknown current distribution. This method eliminates the need of applying boundary conditions to the integral operator and these conditions become a property of the differential equation. Numerical results based on the proposed method show a rate of convergence much faster than that of the classical Pocklington's formulation when simple point matching technique in conjunction with pulse functions is used as a method of solution for the integral equations. The flexibility of the Pocklington's integral equation is still retained. The method is therefore efficient for computation, yielding small matrix to invert, and providing simple expressions for the radiated fields.

ACKNOWLEDGEMENTS

The author is very grateful to his supervisor, Dr. J. Walsh, Associate Professor, Faculty of Engineering and Applied Science, for his excellent guidance and continuous follow-up during the course of this study. His personal involvement, patience and understanding helped in completing this investigation in its present form in a relatively short period.

Special thanks are due to Dean F. Aldrich, School of Graduate Studies, for providing financial assistance and helping immensely in securing teaching assistantships. The excellent facilities provided by Dean R.T. Dempster, Faculty of Engineering and Applied Science is gratefully acknowledged.

The author wishes to express his appreciation to Dr. W.J. Vetter, Dr. M.E. El-Hawary, Dr. A. Zielinski, Dr. D. Dunsiger, and Dr. D. Bajzak, Faculty of Engineering and Applied Science, for their constant advice and encouragement.

Last, but not least, thanks are due to G. Somerton and T.W. Bussey, NLCS, for their valuable assistance during computer programming.

TABLE OF CONTENTS

LIST OF FIGURES

FIGURE PAGE

LIST OF SYMBOLS

$\bar{A}$	Magnetic vector potential
a	Radius of the element
Bin	Input susceptance
$\bar{E}$	Electrical field strength
E_z	Axial component of the electrical field
E_ρ	Radial component of the electrical field
E_ϕ	Angular component of the electrical field
E_z^s	Axial component of the scattered electrical field
E_z^i	Axial component of the incident electrical field
Gin	Input conductance
G(z/z')	Green's function
$\bar{H}$	Magnetic field strength
I_z	Axial component of the current
$\bar{J}$	Current density
J_z	Axial component of the current density
J_ρ	Radial component of the current density
J_ϕ	Angular component of the current density
K_z	Exact kernel for axial field
K_{za}	Approximate kernel for axial field
K_{zc}	Exact composite kernel for axial field
K_{zac}	Approximate composite kernel for axial field
K_ρ	Exact kernel for radial field
$K_{\rho a}$	Approximate kernel for radial field

$K_{\rho c}$	Exact composite kernel for radial field
$K_{\rho ac}$	Approximate composite kernel for radial field
k	Wave number. $(=\omega\sqrt{\mu\epsilon})$
L	Half length of the element
mA/V	Current in milliamperes per unit volt
Rin	Input resistance
T	Linear differential operator $(\nabla\nabla\cdot+k^2)$
T_z	Linear differential operator $(\frac{d^2}{dz^2}+k^2)$
V	Scalar potential
Xin	Input reactance
$\bar{x}$	General R^3 coordinate (x,y,z)
Yin	Input admittance
Zin	Input impedence
(z,ρ,ϕ)	Cylindrical coordinate variables
η_o	Intrinsic impedence of the free space
μ	Permeability of the medium
ϵ	Permittivity of the medium
ω	Radian frequency
$\bar{\nabla}$	Del operator
δ	Dirac-delta function
λ	Wave length
ρ_c	Charge density
*	Convolution

Other symbols are defined as they occur.

CHAPTER 1

INTRODUCTION

1.1 General

There are at present two integral equation formulations in use for the analysis of linear antenna systems. These are the Pocklington's and Hallen's formulations, respectively[1,2,3,4]. Both these formulations have been used extensively by many workers, particularly Hallen's formulation. The latter has been studied in great depth and extended by King[5,6,7]. A good summary of various works related to Hallen's formulation has been given by King[8]. Mie[3] has extended this formulation to an antenna of arbitrary geometry. The more extensive use of Hallen's formulation compared to Pocklington's is because the kernel involved in the integral equation of the former is of a lower order in the sense of derivatives than in the latter. Therefore singularities are less of a problem in Hallen's equation. On the other hand, Hallen's formulation mostly uses a delta-gap generator and does not have the flexibility for ease in handling arbitrary incident fields while Pocklington's formulation has. Therefore Pocklington's equation is more useful in analyzing arbitrary configurations of linear elements.

1.2 Scope of this Thesis

This thesis proposes an alternative to the above classical formulations. The method, which has been discussed previously for the dipole antenna by Walsh[9,10,11], is based on the fact that the radiated electrical field from a current source is given by the product of two linear operators on the expression for the current. One of these is a convolution and the other a differential operator; further, these operators commute in the sense of generalized functions[12]. In the case of a linear antenna the differential operator is invertible in closed form and may be replaced by an intermediate function. The problem of determining unknown expressions for currents on an antenna system subjected to some known incident field may then be solved by first finding the solution of an integral equation for the intermediate function, after which expressions for unknown currents may be found by a simple integration. The kernel of the integral equation used in this method is similar to that of Hallén's equation and at the same time the flexibility of Pocklington's formulation is retained.

Any of the standard numerical techniques[13,14,4], such as Galerkin's method, point matching, and best approximation may be used to solve the integral equation in conjunction with a variety of approximating functions for the unknown of the equation. For comparison with available

results for convergence with Pocklington's equation, using the point matching technique in conjunction with pulse functions, the same technique has been used to solve the integral equation based on the proposed method. The results contained in this thesis show a much faster rate of convergence compared to results for Pocklington's equation, and are comparable when entire domain cosine mode functions are used instead of pulse functions in Pocklington's equation. For all further computations also, the numerical technique used is again point matching in conjunction with pulse functions. This choice is made because of the attached simplicity and convenience with this technique for the cases considered. The results include input impedence and current distributions for the linear dipole antenna. For examples of multi-element structures a V-antenna[15], and top loaded antenna[16] are solved for input impedence and current distributions. The results are compared with measured results and the agreement is good in general.

CHAPTER 2

THE GENERAL FORMULATION

Assume a current source $\bar{J}(\bar{x})$, existing only in a bounded region of three dimensional space R^3, and immersed in an infinite nonconductive, isotropic, homogeneous medium with permeability μ and permittivity ε. For the steady state sinusoidal case the Helmholtz equation for the vector potential $\bar{A}(\bar{x})$ can be written as (see Appendix A.1)

$$\bar{\nabla}^2\bar{A}(\bar{x}) + k^2\bar{A}(\bar{x}) = -\mu\bar{J}(\bar{x}) \qquad (2.1)$$

where $\bar{x}$ is the general R^3 coordinate (x,y,z) and $k = \omega\sqrt{\mu\varepsilon}$ is the wave number with ω as radian frequency. The fundamental scalar solution of (2.1) subject to the radiation condition at infinity, that is the field has outward traveling condition at infinity, is given by[17]

$$K(\bar{x}) = \frac{\exp[-jkr(\bar{x})]}{4\pi r(\bar{x})}, \qquad (2.2)$$

$$r(\bar{x}) = (x^2 + y^2 + z^2)^{\frac{1}{2}} \qquad (2.3)$$

That is, $K(\bar{x})$ is the solution of the scalar equation

$$\bar{\nabla}^2 f(\bar{x}) + k^2 f(\bar{x}) = -\delta(\bar{x}) \qquad (2.4)$$

where $f(\bar{x})$ is a scalar function and

$\delta(\bar{x})$ is the three dimensional Dirac-delta function.

The solution of equation (2.1) is then

$$\bar{A}(\bar{x}) = \mu\bar{J}(\bar{x}) * K(\bar{x}) \tag{2.5}$$

where * denotes componentwise convolution in R^3. Equation (2.5) is written in the sense of generalized functions[12]. In this sense it is well defined since $\bar{J}(\bar{x})$ only exists in a bounded region and is at least continuous, and $K(\bar{x})$ is locally integrable in R^3.

The radiated electrical field intensity $\bar{E}(\bar{x})$ is related to $A(\bar{x})$ by (see equation (A.9))

$$\bar{\nabla}x\bar{\nabla}x\bar{A}(\bar{x}) = j\mu\omega\varepsilon\bar{E}(\bar{x}) + \mu\bar{J}(\bar{x}). \tag{2.6}$$

Combining equations (2.6) and (2.1) and by using the vector identity

$$\bar{\nabla}x\bar{\nabla}x\bar{A}(\bar{x}) = \bar{\nabla}\bar{\nabla}\cdot\bar{A}(\bar{x}) - \bar{\nabla}^2\bar{A}(\bar{x}) \tag{2.7}$$

$\bar{E}(\bar{x})$ can be given as

$$\bar{E}(\bar{x}) = \frac{1}{j\omega\mu\varepsilon}\left[\bar{\nabla}\bar{\nabla}\cdot\bar{A}(\bar{x}) + k^2\bar{A}(\bar{x})\right] \tag{2.8}$$

$$= \frac{1}{j\omega\mu\varepsilon}T[\bar{A}(\bar{x})] \tag{2.9}$$

where T is the linear differential operator $(\bar{\nabla}\bar{\nabla}\cdot + k^2)$. Applying equation (2.9) to (2.5) yields (2.10a) and hence (2.10b) for $\bar{E}(\bar{x})$, since convolution commutes with differentiation in the sense of generalized functions[12].

$$\bar{E}(\bar{x}) = T[\bar{J}(\bar{x}) * K_o(\bar{x})] \qquad (2.10a)$$

$$= T[\bar{J}(\bar{x})] * K_o(\bar{x}) \qquad (2.10b)$$

where

$$K_o(\bar{x}) = K(\bar{x})/j\omega\varepsilon \qquad (2.11)$$

It can be seen that if $\bar{x}$ in equations (2.10) is normalized to wavelength as,

$$\bar{x}_o = \bar{x}/\lambda \qquad (2.12)$$

Then T and K_o are given as

$$T_{\bar{x}_o} = (\bar{\nabla}\bar{\nabla}_{\bar{x}_o} \cdot + 4\pi^2) \qquad (2.13)$$

$$K_o(\bar{x}_o) = (\mu/\varepsilon)^{\frac{1}{2}} \frac{\exp[-j2\pi r(\bar{x}_o)]}{j\,8\pi^2 r(\bar{x}_o)} \qquad (2.14)$$

where $T_{\bar{x}_o}$ refers to the operator T with respect to $\bar{x}_o$, and $\bar{\nabla}\bar{\nabla}_{\bar{x}_o}\cdot$ refers to $\bar{\nabla}\bar{\nabla}\cdot$ with respect to $\bar{x}_o$. For this normalization the current density $\bar{J}$ should be expressed in amperes/(wavelength)^2 and the resulting electrical field E is in terms of volt/wavelength. The convolution in equations (2.10) is with respect to $\bar{x}_o$, i.e. $\bar{x}/\lambda$.

It should be noted that equation (2.10b) may be obtained directly from Maxwell's equations and the equation of continuity without using the concept of vector potential as shown in Appendix A.2 and hence (2.10a), since (2.10a) follows from (2.10b) equally as well as (2.10b)

from (2.10a).

Equation (2.10) is the starting point for several methods of analysis of antenna problems. It should be noted that Hallen's integral equation is derived from equation (2.10a). Either of the forms of (2.10) may be used to determine unknown current densities on some body subjected to known incident electric field intensities or vice versa. However, since physical properties of the body usually impose boundary conditions on the current densities it appears more convenient to use (2.10b) when possible.

Consider, for example, the case of a perfectly conducting body with known incident fields $\bar{E}^i(\bar{x})$ over its surface, i.e., $\bar{E}^i(\bar{x})$ is the electrical field from some external source. The problem of determining the surface current densities $\bar{J}_s$ amounts to finding a solution of the differential equation $T(\bar{J}_s)$ such that $\bar{J}_s$ satisfies the physical boundary conditions imposed by the conductor. Let the convolution be

$$\bar{f}(\bar{x}) * K_o(\bar{x}) = T_K(\bar{f}) \tag{2.15}$$

then the set of all radiated fields from the conductor is given by

$$\bar{E}(\bar{x}) = T_K(T(\bar{J}_s)) \tag{2.16}$$

where $\bar{J}_s$ ranges over the set of all current densities which satisfy the boundary conditions imposed by the conductor. Since a perfect conductor cannot support the tangential component of any electrical field over its surface, it follows

$$\bar{E}_t(\bar{x}) + E^i_t(\bar{x}) = 0 \tag{2.17}$$

where t refers to the tangential component of the fields. The problem above then may be stated as that of inverting the composite operator $T_K T$ for the given incident field. This may be accomplished by restricting the convolution T_K to the conductor surface, i.e.,

$$T_{Ks}(T(\bar{J}_s)) = -E^i_t(\bar{x}) \tag{2.18}$$

where T_{Ks} is the restriction of T_K and solving the differential equation

$$T(\bar{J}_s) = T^{-1}_{Ks}\,[-E^i_t\,(\bar{x})] \tag{2.19}$$

where T^{-1}_{Ks} is the inverse of T_{Ks}, provided of course this inverse exists.

It should be noted that equations (2.10) state that T and T_K commute, i.e.,

$$T(T_K(\bar{J}_s)) = T_K(T(\bar{J}_s)) \tag{2.20}$$

Equations (2.10) are written in the sense of generalized functions thus, for some current distributions $T(\bar{J})$ may contain singularity functions, i.e., the delta function and even its derivative. The later is unlikely in a practical sense, however, since it implies a discontinuous current.

It is of interest to note that in the case of a linear antenna the differential operator T is invertible in closed form. Thus, for the known incident field the inverse

convolution operator T_K^{-1} may be obtained by using any standard method of solving integral equations and current distributions can be determined from closed form solution of the differential operator T. This case is discussed in the next two chapters.

CHAPTER 3

LINEAR CYLINDRICAL DIPOLE ANTENNA

3.1 The Basic Linear Element

Consider a linear cylindrical tube of radius a and length 2L satisfying the following usual assumptions for such an element:

(a) The tube is a thin walled perfect conductor.

(b) It carries a current along the longitudinal direction only and confined to the surface.

(c) The radius of the tube is much smaller than the operating wavelength, so the current may be assumed to be distributed uniformly over the tube.

The axis of the tube coincides with the z axis of the cylindrical coordinate (z,ρ,ϕ) and center at the origin. The current distributions for the tube thus can be given as,

$$J_\rho = J_\phi = 0$$

$$J_z = \frac{I_z(z)}{2\pi a}\,\delta(\rho-a) \quad \text{for} \quad -L\le z\le L \qquad (3.1)$$

$$J_z = 0 \quad \text{for} \quad |z|>L$$

where δ is the Dirac-delta function and ρ is cylindrical radial distance variable. This is the usual model of a

basic linear element acting as a current source for equations (2.10).

It is shown in Appendix B that from equations (2.10) the radiated electrical field from such a source is given by

$$E_z(z,\rho) = T_z[I_z(z)] * K_z(z,\rho) \tag{3.2}$$

$$E_\rho(z,\rho) = -T_z[I_z(z)] * K_\rho(z,\rho) \tag{3.3}$$

$$E_\phi = 0 \tag{3.4}$$

where E_z, E_ρ and E_ϕ are axial, radial, and angular components of the electrical field respectively, and

$$T_z = \left(\frac{d^2}{dz^2} + k^2\right) \tag{3.5}$$

$$K_z(z,\rho) = \frac{1}{2\pi}\int_o^{2\pi} K_o(z,\rho,\phi)\,d\phi \tag{3.6}$$

$$K_\rho(z,\rho) = \frac{1}{2\pi}\int_o^{2\pi} \frac{z(\rho - a\cos\phi)}{\rho^2 + a^2 - 2\rho a\cos\phi} K_o(z,\rho,\phi)\,d\phi \tag{3.7}$$

where $K_o(z,\rho,\phi)$ is given by

$$K_o(z,\rho,\phi) = \frac{\exp[-jkr(z,\rho,\phi)]}{j4\pi\omega\varepsilon r(z,\rho,\phi)} \tag{3.8}$$

with $r(z,\rho,\phi) = (z^2 + \rho^2 + a^2 - 2\rho a\cos\phi)^{\frac{1}{2}}$

and the convolution in (3.2) and (3.3) is restricted to z only.

3.1.1 The Differential Operator for the Linear Element

Let us now consider the differential operator

$$T_z[I_z] = \frac{d^2 I_z}{dz^2} + k^2 I_z \qquad (3.9)$$

appearing in equations (3.2) and (3.3). This operator should be defined for all z, i.e., $-\infty<z<\infty$. The support of I_z, however, is the interval [-L, L], i.e., $I_z = 0$ for $|z|>L$.

Consider first the restriction of $T_z[I_z]$ to the interval [-L, L]. Let us set this restriction equal to some auxiliary function, say $E_o(z)$, i.e.,

$$T_z(I_z) = \frac{d^2 I_z}{dz^2} + k^2 I_z = E_o(z) \quad -L\leq z\leq L \qquad (3.10)$$

This restriction is now extended to the entire real line by setting

$$E_o(z) = 0, \quad |z|>L \qquad (3.11)$$

with the result

$$T_z(I_z) = E_o(z) + I_z(-L)\delta'(z+L) - I_z(L)\delta'(z-L) + I_z'(-L)\delta(z+L) - I_z'(L)\delta(z-L) \qquad (3.12)$$

where $I_z(-L)$ and $I_z(L)$ are the currents at the ends $z = -L$ and $z = L$ respectively, and primes denote differentiation with respect to z. $I_z'(-L)$ and $I_z'(L)$ are the limiting values

at -L and L inside the interval [-L, L], i.e.,

$$I'_z(-L) = \lim_{z \to -L_+} I'_z(z) \quad \text{from } -L_-$$

$$I'_z(L) = \lim_{z \to L_+} I'_z(z) \quad \text{from } L_- \tag{3.13}$$

Consider now the differential equation

$$\frac{d^2 I_z}{dz^2} + k^2 I_z = E_o(z) \quad , \quad -L \leq z \leq L \tag{3.14}$$

This equation may be solved subject to some boundary conditions on the current. Let these boundary conditions be the end currents $I_z(-L)$ and $I_z(L)$. Then the solution is

$$I_z(z) = I_z(-L) \frac{\sin[k(L-z)]}{\sin(2kL)} + I_z(L) \frac{\sin[k(L+z)]}{\sin(2kL)}$$

$$+ \int_{-L}^{L} G(z/z') E_o(z') dz' \tag{3.15}$$

where $G(z/z')$ is the Green's function given by

$$G(z/z') = -\begin{cases} \dfrac{\sin[k(L+z)]\sin[k(L-z')]}{k \sin(2kL)}, & z<z' \\ \dfrac{\sin[k(L-z)]\sin[k(L+z')]}{k \sin(2kL)}, & z>z' \end{cases} \tag{3.16}$$

This solution is subject to the condition $\sin(2kL) \neq 0$, i.e., $L \neq n\lambda/4$, where λ is the wavelength and n a positive integer. The case $\sin(2kL) = 0$ has been treated in the literature[11]. However, in practical cases the situation of this singularity can be avoided by treating the element of singular Green's function length as two different elements axially joined together in a straight line. The lengths of each are such that the Green's function is not singular. Examples of this case are given in the section on dipole antenna.

Equations (3.2) and (3.3) for the radiated field may now be written as

$$E_z(z,\rho) = \int_{-L}^{L} E_o(z')\, K_{zc}(z/z'/\rho)\, dz' + I_z(-L)\, K'_z(z+L,\rho) - I_z(L)\, K'_z(z-L,\rho) + b\, K_z(z+L,\rho) - c\, K_z(z-L,\rho) \quad (3.17)$$

$$E_\rho(z,\rho) = -\left[\int_{-L}^{L} E_o(z') K_{\rho c}(z/z'/\rho)\, dz' + I_z(-L)\, K'_\rho(z+L,\rho) - I_z(L)\, K'_\rho(z-L,\rho) + b\, K_\rho(z+L,\rho) - c\, K_\rho(z-L,\rho)\right] \quad (3.18)$$

where the primes denote differentiation with respect to z and

$$K_{zc}(z/z'/\rho) = K_z(z-z',\rho) + K_z(z+L,\rho)G'(-L/z') - K_z(z-L,\rho)G'(L/z') \quad (3.19)$$

$$K_{\rho c}(z/z'/\rho) = K_\rho(z-z',\rho) + K_\rho(z+L,\rho)G'(-L/z') - K_\rho(z-L,\rho)G'(L/z') \quad (3.20)$$

$$b = -I_z(-L)\frac{k\cos(2kL)}{\sin(2kL)} + I_z(L)\frac{k}{\sin(2kL)} \quad (3.21)$$

$$c = -I_z(-L)\frac{k}{\sin(2kL)} + I_z(L)\frac{k\cos(2kL)}{\sin(2kL)} \quad (3.22)$$

$$G'(-L/z') = -\frac{\sin[k(L-z')]}{\sin(2kL)}, \quad z'>-L \quad (3.23)$$

$$G'(L/z') = \frac{\sin[k(L+z')]}{\sin(2kL)}, \quad z'<L \quad (3.24)$$

Equations (3.15), (3.17), and (3.18) may be used as a basis for the analysis of thin, tubular, linear antenna systems. For if the scattered electrical field E_z^s is specified, equation (3.17) may be solved for $E_o(z')$ and the end currents $I_z(L)$ and $I_z(-L)$, and the antenna current may be determined from equation (3.15).

It should be noted that Hallen's equation[2] for this problem is the result of applying (2.10a), while Pocklington's equation results when the operator T_z, given by (3.5), is applied to K_z instead of I_z in (3.2). These two classical formulations will again be discussed briefly for the case of a dipole in the next section.

3.2 The Dipole Antenna: Current and Impedence

3.2.1 The Dipole

In this section attention will be confined to the simple cylindrical dipole antenna in free space of length 2L and radius a centered at the origin. The axis of the dipole coincides with the z axis as shown in Figure 3.1. Again the usual assumptions are made for the dipole the same as are made for the basic linear element in Section 3.1. The dipole is center driven by a magnetic frill current source[4,18] as opposed to the delta gap voltage generator used extensively by other workers. This choice is made because this is a comparatively better model of an actual physical situation, e.g., when an antenna over a ground plane is fed through a coaxial cable. The ratio of outer to inner radius of the frill is taken 2.23, since this gives a characteristic impedence of an airfilled coaxial cable of 50 ohms. This is a standard impedence of a cable normally used in feeding such antennas.

3.2.2 The Approximate Kernel

Considerable simplification is achieved in solving linear antenna problems by adopting the practice of using an approximate kernel[4,19,20] in equation (3.2). Thus $K_z(z,\rho)$ in (3.2) is replaced by

$$K_{za}(z,\rho) = \frac{\exp[-jk(z^2+\rho^2+a^2)^{\frac{1}{2}}]}{j4\pi\omega\epsilon(z^2+\rho^2+a^2)^{\frac{1}{2}}} \qquad (3.25)$$

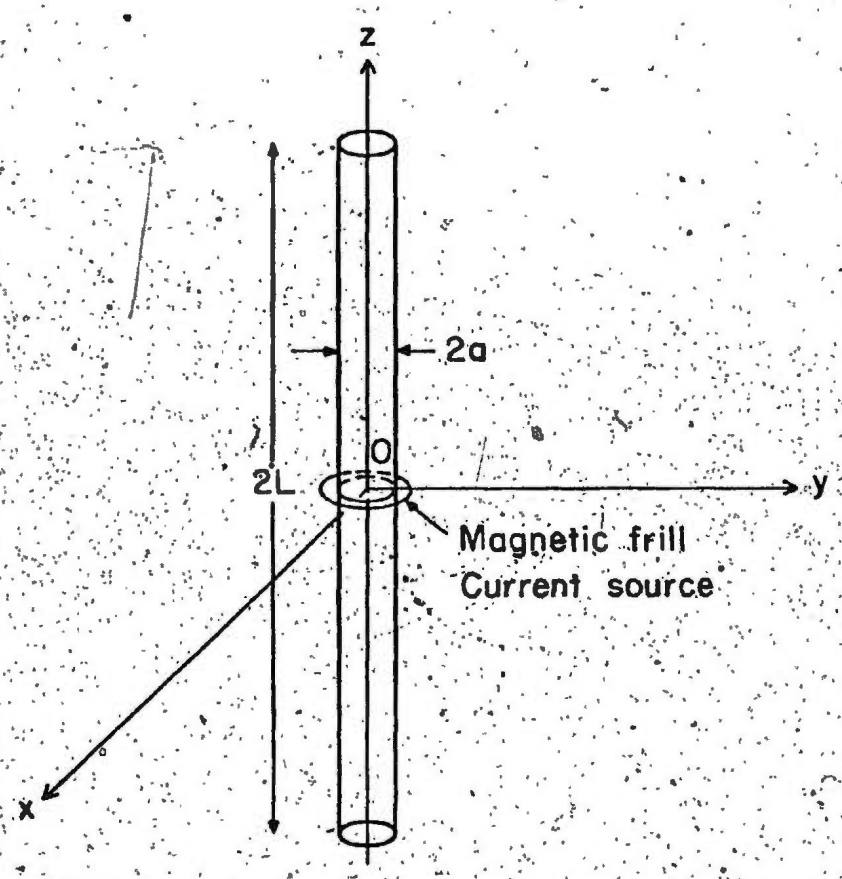

Figure 3.1. Geometry of a symmetrical center-fed linear cylindrical dipole.

Further for the case of a dipole ρ equals 0 in calculating the scattered field. An interpretation of this is that the observation point for the field lies on the axis and the surface current distribution is represented by an equivalent filamentary line source, parallel to the axis and located at a radial distance a from it. Thus, equation (3.25) reduces to

$$K_{za}(z,0) = \frac{\exp[-jk(z^2+a^2)^{\frac{1}{2}}]}{j4\pi\omega\varepsilon(z^2+a^2)^{\frac{1}{2}}} \tag{3.26}$$

The above is the same approximate kernel given by King[5-8] and Mie[3] for this case.

Before applying the particular formulation discussed in Section (3.1) to the present dipole and multi-wire structures in Chapter 4, two classical formulations, Hallen's and Pocklington's, will be discussed briefly for the dipole of this section.

3.2.3 Hallen's Integral Equation

As pointed out earlier, Hallen's equation can be derived from equation (2.10a). This equation is used extensively by many workers, particularly by King[5-8] and also by Mie[3] who extended it to antennas of arbitrary shape. For the case of a dipole and by using the approximate kernel of (3.26) for the scattered field, equations (2.10a) through (3.2) reduces to

$$E_z^s(z,0) = T_z[I_z(z) * K_{za}(z,0)] \tag{3.27}$$

where T_z is given by equation (3.5) and convolution is restricted to z only. If the antenna is driven at the center by a delta-gap voltage generator V such that the axial component of incident field is given by

$$E_z^i(z,0) = V\delta(z) \tag{3.28}$$

the equation (3.27) becomes

$$T_z[I_z(z) * K_{za}(z,0)] = -V\delta(z) \tag{3.29}$$

and further solving for $I_z * K_{za}$ yields

$$\int_{-L}^{L} I_z(z') K_{za}(z-z',0)\,dz'$$

$$= \frac{j}{2\eta_o}(C\cos kz + V\sin k|z|) \tag{3.30}$$

where η_o is the free space intrinsic impedence. This is Hallen's integral equation for the simple dipole. The constant C must be evaluated from the condition that the current vanishes at both ends of the antenna.

3.2.4 Pocklington's Integral Equation

Pocklington's integral equation results when the operator T_z is applied to K_{za} instead of I_z in equation (3.2). This application for the dipole gives the scattered field as

$$E_z^s(z,0) = I_z(z) * T_z[K_{za}(z,0)] \tag{3.31}$$

Where T_z is given by equation (3.5) and convolution is again restricted to z only. For the known incident field E_z^i, equation (3.31) becomes

$$I_z * T_z[K_{za}(z,0)] = -E_z^i(z,0) \tag{3.32}$$

or

$$\int_{-L}^{L} I_z(z')\left[\frac{d^2}{dz^2} K_{za}(z-z',0) + k^2 K_{za}(z-z',0)\right]dz' = -E_z^i(z,0) \tag{3.33}$$

The above equation is of the form given by Pocklington to solve for current distributions on thin wire antenna. This equation is also used extensively by many workers to solve various antenna problems. The equation is more flexible than Hallen's in the sense that it can easily handle an arbitrary incident field which is advantageous in analyzing multi-wire structures.

The composite kernel K_{zc}, or its approximate K_{zac} obtained by replacing K_z by K_{za} in equation (3.19) of K_{zc}, of the integral equation based on the proposed method is of the same lower order as the kernel K_z or K_{za} of Hallen's integral equation, in the sense that they do not involve derivatives of the kernel K_z, or of its approximate K_{za}. Also, the composite kernel K_{zc} or K_{zac} goes to zero at $z' = -L$ and L for all z except possibly for $z = -L$ and L, whereas Hallen's kernel does not. In this sense it appears that the composite kernel in the proposed method is better behaved than Hallen's kernel. In the case of Pocklington's integral equation the derivative of the current is transferred to the kernel K_z or K_{za}. The resulting kernel is

therefore of a higher order than the kernels of other two integral equations. Hence, singularities in the kernel are more of a problem in Pocklington's equation than in Hallén's equation or the equation based on the proposed method.

3.2.5 Solution for the Current

Using the approximate kernel of equation (3.26) and conditions $I_z(-L) = I_z(L) = 0$, equations (3.17) and (3.15) reduce to

$$\int_{-L}^{L} E_o(z')K_{zac}(z/z'/0)\,dz' = -E_z^i(z,0) \qquad (3.34)$$

and

$$I_z(z) = \int_{-L}^{L} G(z/z')E_o(z')dz' \qquad (3.35)$$

where $E_z^i(z,0)$ is a given axial incident field and K_{zac} is given by equation (3.19) with the change that $K_z(z,\rho)$ is replaced by the approximate kernel $K_{za}(z,0)$.

The approximate current distribution for the dipole may thus be obtained, and hence input impedence, by first finding $E_o(z')$ from equation (3.34) and then solving (3.35) for $I_z(z)$. Any of the standard techniques may be used for solving (3.34), such as method of moments. This method is discussed in the next section.

3.2.6 Method of Moments

One of the standard numerical techniques used in solving an integral equation is method of moments[13]. An

important class of this method is that characterized by various titles: Rayleigh-Ritz, Galerkin or variational method. These techniques are widely used to solve the integral equation occurring in electromagnetic field problems and in this area it is more known as reaction concept[14,21]. The general approach to solve problems is usually a reduction of the associated integral equation to a system of N linear algebric equation in N unknowns, where the N unknowns are generally coefficients in some suitable expansion of the unknown function of the equation, e.g., $E_o(z')$ in equation (3.34).

Equation (3.34) in an operator form can be written as

$$S[E_o] = -E_z^i \qquad (3.36)$$

where S is linear integral operator, E_z^i is known, and E_o is to be determined. The definition of S is obvious from (3.34) i.e.,

$$S[E_o] = \int_{-L}^{L} E_o(z') K_{zac}(z/z'/0) dz' \qquad (3.37)$$

Let E_o be expanded in a series of functions, E_{o1}, E_{o2}, E_{o3}, . . . in the domain of S, as

$$E_o = \sum_{j=1}^{n} g_j E_{oj} \qquad (3.38)$$

the coefficients g_j's are constants. The E_{oj}'s are called expansion functions or basis functions. For exact solution n is usually infinite. For approximate solution n is finite,

i.e., the summation in (3.38) is truncated. The g_j's are now the unknowns that have to be determined. Substitution of (3.38) in (3.36) yields

$$S\left[\sum_{j=1}^{n} g_j E_{oj}\right] = -E_z^i \qquad (3.39)$$

using the linearity of S,

$$\sum_{j=1}^{n} g_j S[E_{oj}] = -E_z^i \qquad (3.40)$$

It is often necessary to define a suitable inner product $\langle E_o, E_z \rangle$ (in electromagnetic field problems this is called reaction). A suitable inner product for such problems is defined by[4, 14].

$$\langle E_o, E_z \rangle = \int_{-L}^{L} E_o(z) E_z(z) dz \qquad (3.41)$$

Now, let us define a set of weighting functions, also called testing functions, $W_1, W_2, W_3 \ldots W_m$, and form the inner product for each W_i. This yields

$$\sum_{j=1}^{n} g_j \langle W_i, S[E_{oj}] \rangle = -\langle W_i, E_z^i \rangle \qquad (3.42)$$

where $i = 1, 2, 3 \ldots m$. This set of equations for $m = n$, can be written in the matrix form as

$$\begin{bmatrix} \langle W_1, S[E_{o1}]\rangle & \langle W_1, S[E_{o2}]\rangle & \cdots & \langle W_1, S[E_{on}]\rangle \\ \langle W_2, S[E_{o1}]\rangle & \cdots & & \\ \vdots & & & \\ & & & \langle W_n, S[E_{on}]\rangle \end{bmatrix} \begin{bmatrix} g_1 \\ g_2 \\ \vdots \\ g_n \end{bmatrix}$$

$$= - \begin{bmatrix} \langle W_1, E_z^i\rangle \\ \langle W_2, E_z^i\rangle \\ \vdots \\ \langle W_n, E_z^i\rangle \end{bmatrix} \tag{3.43}$$

Equation (3.43) can be solved by any standard matrix inversion technique for unknown column vector g_j provided this inverse exists. It is to be noted that if weighting functions W_i's are taken equal to basis functions E_{oj}'s, it is known as Galerkin's method. In using the above technique for solving the problem it is important to have proper choice of the basis functions E_{oj}'s in the sense that these should be linearly independent and can approximate $E_o(z)$ reasonably well through some superposition like (3.38). This, in general, gives faster convergence which means

the size of smaller matrix to calculate and invert in equation (3.43). Also, in some cases, this realizes a better conditioned matrix.

There are two classes of basis functions, namely entire domain bases and subdomain bases. Entire domain bases exist over complete domain of integral operator S. Subdomain bases exist only over part of domain S, otherwise zero. This constitutes dividing the antenna into segments or subsections, and thus each g_j of the expansion (3.38) affects the approximation of $E_o(z)$ only over a subsection of the region of interest. Some common basis functions used in wire antenna problems are given in the literature (4). A few of them are as follows:

(a) Entire domain bases

(i) Fourier: $E_o(z) = g_1 \cos(\pi z/2L) + g_2 \cos(3\pi z/2L) + g_3 \cos(5\pi z/2L) + \ldots$ (3.44)

(ii) Maclaurin: $E_o(z) = g_1 + g_2(z/L)^2 + g_3(z/L)^4 + \ldots$ (3.45)

(b) Subdomain bases

(i) Pulse function (piecewise uniform):

$$E_o(z) = \begin{cases} g_j & \text{for } z \text{ in } \Delta z_j \\ o & \text{otherwise} \end{cases} \qquad (3.46)$$

(ii) Triangle function (piecewise linear):

$$E_o(z) = \begin{cases} \dfrac{g_j(z_{j+1}-z) + g_{j+1}(z-z_j)}{\Delta z_j} & \text{for } z \text{in} \Delta z_j \\ 0 \quad \text{otherwise} \end{cases} \tag{3.47}$$

3.2.6-1 Point Matching

The calculation of matrix elements in equation (3.43) is quite often tedious, since it requires two integrations per element, one because of an integral operator S and the other in the evaluation of an inner product. Moreover, most of the time they have to be done numerically. This is very time-consuming even on high speed digital computers. The trouble can be reduced if the choice for weighting function W_i is taken to be Dirac-delta function. This eliminates one integration per element. For this choice of W_i, equation (3.39) can be written as

$$\begin{bmatrix} \langle\delta(z-z_1),\ S[E_{o1}]\rangle & \langle\delta(z-z_1),\ S[E_{o2}]\rangle & \cdots \\ \langle\delta(z-z_2),\ S[E_{o1}]\rangle & & \\ \vdots & & \\ & & \langle\delta(z-z_n),\ S[E_{on}]\rangle \end{bmatrix} \begin{bmatrix} g_1 \\ g_2 \\ \vdots \\ g_n \end{bmatrix} = - \begin{bmatrix} \langle\delta(z-z_1),\ E_z^i\rangle \\ \langle\delta(z-z_2),\ E_z^i\rangle \\ \vdots \\ \langle\delta(z-z_n),\ E_z^i\rangle \end{bmatrix} \tag{3.48}$$

where δ is Dirac-delta function.

By taking the inner product, equation (3.48) can be simplified as

$$\begin{bmatrix} S_{z_1}[E_{o1}] & S_{z_1}[E_{o2}] & \cdots & S_{z_1}[E_{on}] \\ S_{z_2}[E_{o1}] & \cdots & & \\ \vdots & & & \\ & & & S_{z_n}[E_{on}] \end{bmatrix} \begin{bmatrix} g_1 \\ g_2 \\ \vdots \\ g_n \end{bmatrix} = - \begin{bmatrix} E_z^i(z_1,0) \\ E_z^i(z_2,0) \\ \vdots \\ E_z^i(z_n,0) \end{bmatrix} \tag{3.49}$$

where S_{z_i} is the restriction on S and means that it operates on E_{oj} at a particular z_i and $E_z^i(z_i,0)$ is the axial component of an incident field at that z_i. Any integrations that are needed are now only those due to S_{z_i}. In the above equation the field is matched at discrete points so this technique is known as point matching.

3.2.6-2 Best Approximation Technique

The technique used for solving the integral equation (3.34) by matrix inversion in equations (3.43) or (3.49) can be improved by taking m>n and solve the overdetermined system of linear algebric equations. This technique is known as best approximation technique, and is discussed in Chapter 5 of Delves and Walsh[13]. Under this technique the most appealing type is Chebyshev approximation. The method

is based on linear programming problem. Computer algorithms are available to deal with this method.

3.2.7 Numerical Results and Comparison

This section comprises the numerical results obtained for the dipole in free space and a comparison is made with the results of other workers. Equation (3.34) is solved for $E_o(z')$ using pulse functions given by (3.46), in conjunction with a point matching technique. This particular choice is also made in solving multi-wire structures. This method is selected for comparison with available results for convergence for Pocklington's equation using the same numerical method. Further, this method has other advantages apart from those already discussed for point matching technique. The kernel K_{zac} in equation (3.34) has to be integrated over relatively small length and involves only sine and cosine integrals. The terms resulting from end effects in K_{zac} and the integration of the Green's function $G(z/z')$ in equation (3.35) for the current are in closed form as shown in Appendix (B.4). Also, for that choice the radial field $E_\rho(z,\rho)$ is available in closed form which is important for multi-wire systems. For this choice equations (3.34) and (3.35) can be written as

$$\sum_{j=1}^{n} g_j \int_{q_1}^{q_2} K_{zac}(z_i/z'/0)\,dz' = -E_z^i(z_i,0) \qquad (3.50)$$

$$\text{for } i = 1, 2, \ldots n$$

and

$$I_z(z) = \sum_{j=1}^{n} g_j \int_{q_1}^{q_2} G(z/z')dz' \qquad (3.51)$$

where q_1 and q_2 are the lower and upper limits of $\Delta z'_j$ for j^{th} segment of equation (3.46).

Figure 3.2 shows the input impedence of a dipole calculated by the proposed method for different numbers of segments like (3.46). Also contained in this figure are the results of calculations by Thiele[4] using Pocklington's equation (3.33) and point matching. The same type of functions as (3.46) are used to approximate the current, and the same exciting field, i.e., a magnetic frill current used. It can be seen that convergence is much faster in the proposed method compared with Pocklington's equation. Also, the required integrations are more complex in the latter.

Figure 3.3 shows a second dipole example. A solution of the same problem using Pocklington's equation and entire domain cosine modes, given by equation (3.44), to approximate the current solution are also shown[4]. The rates of convergence are similar but integrations using Pocklington's equation are much more complex and have to be evaluated for the complete length of the dipole. Also plotted in Figure 3.3 are results for the same dipole using Hallen's equation (3.30) and entire domain cosine modes to approximate the current solution.[4] In the latter case, however, a delta-gap

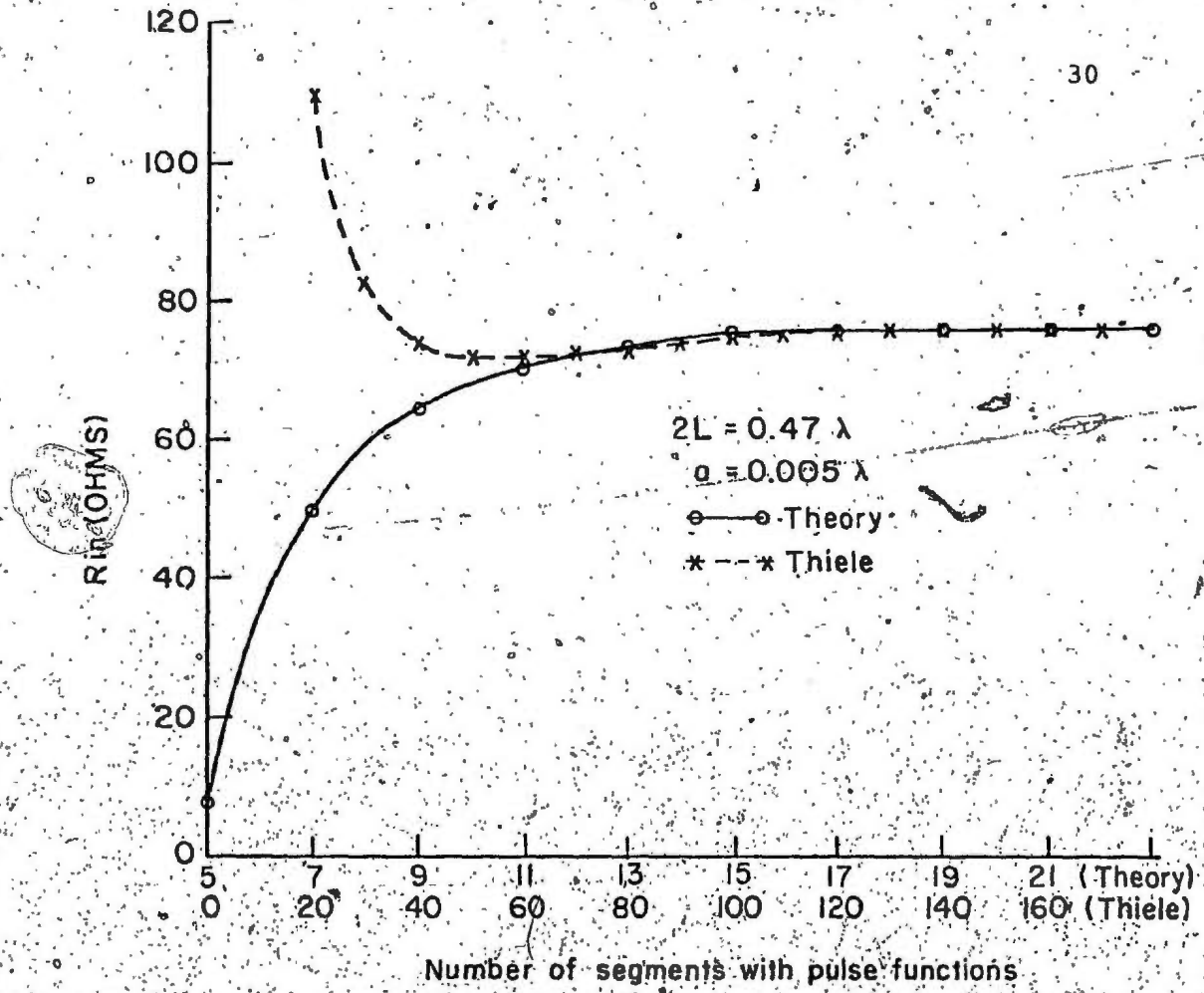

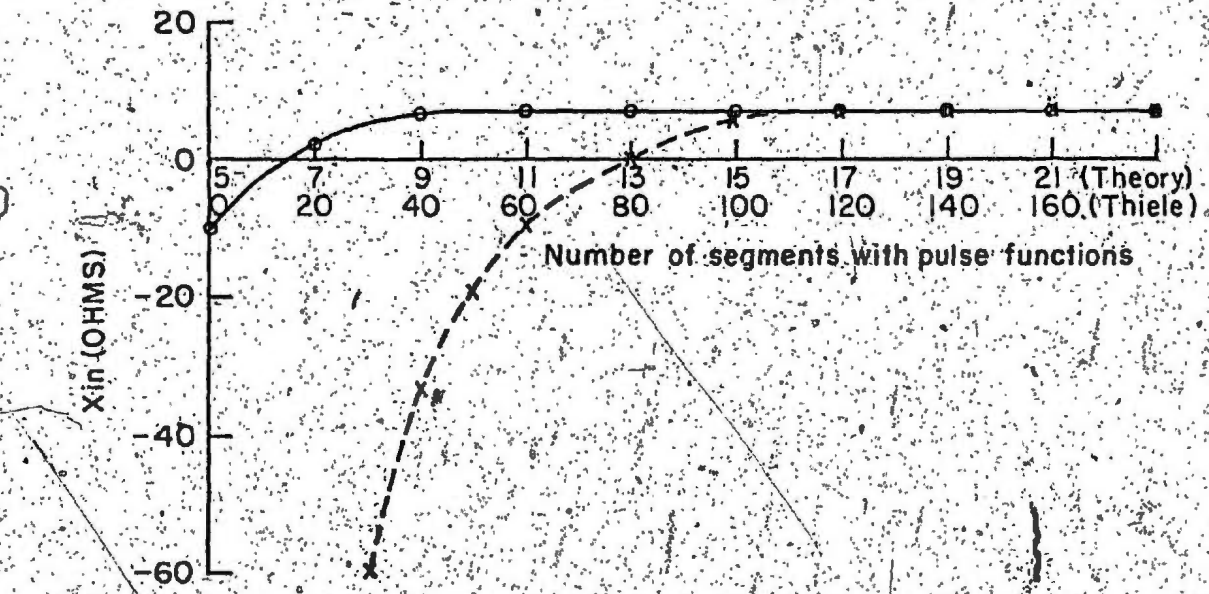

Figure 3.2. Curves showing convergence of input impedence of a center-fed dipole antenna.

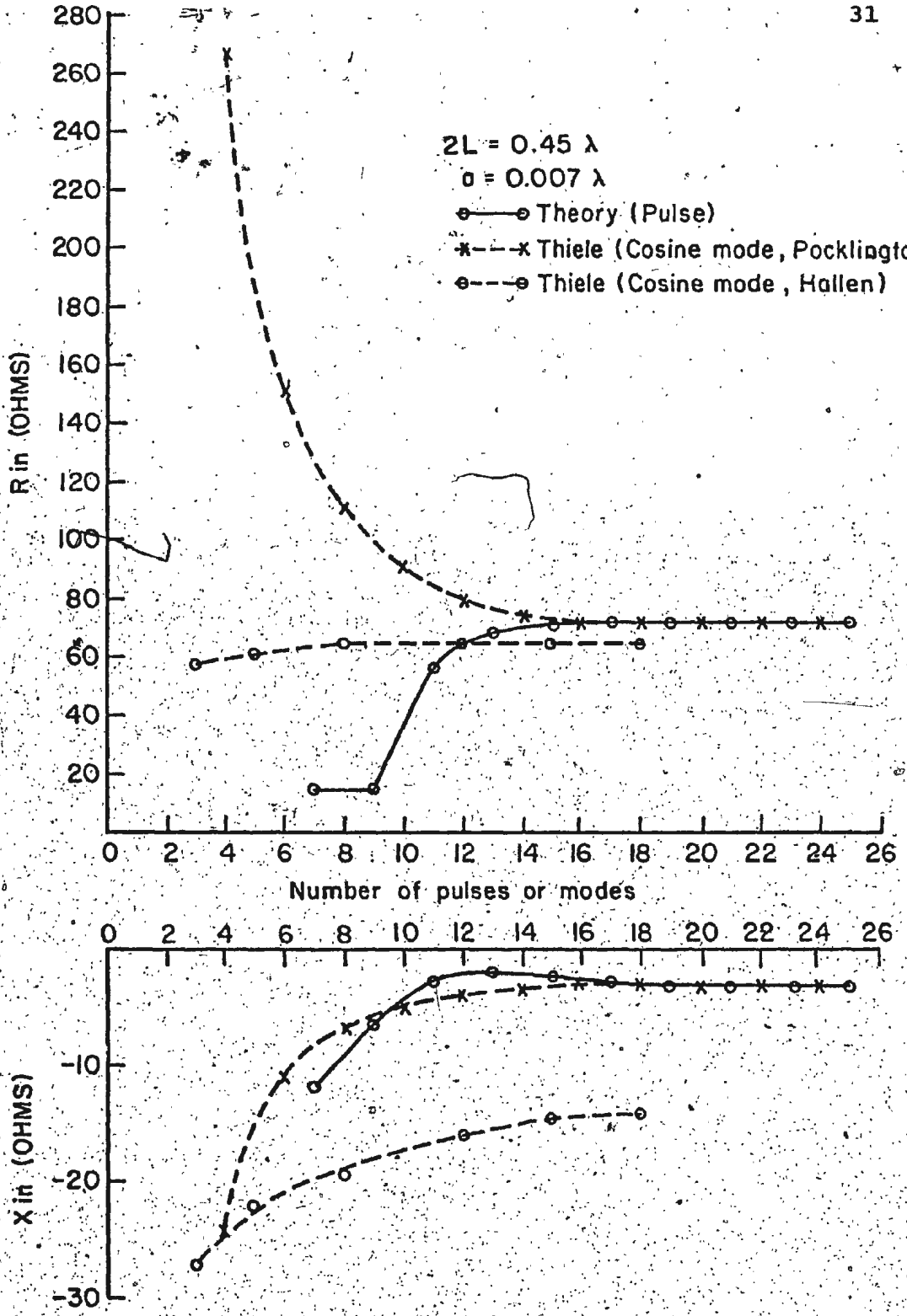

Figure 3.3. Curves showing convergence of input impedence of a center-fed dipole antenna.

generator is used as a field source. No direct comparison is possible since in this case the impedence converges to a different value, however the rates of convergence may be seen to be similar, although again the integrations are more complex and have to be evaluated for the complete length of the dipole.

It should be noted that in the method used the current is not approximated but $T_z(I_z)$, hence, simpler approximating functions may be tolerated. It is readily checked that using the functions of (3.46) to approximate E_o gives rise to a current which has a continuous first derivative. On the other hand, if functions like (3.46) are used to approximate the current higher order fields involving the second derivative of the kernel in equation (3.33) are generated. Hence, for "normal" exciting fields simple approximating functions for the current cannot be expected to give good results.

Figure 3.4 shows the input admittance for different lengths of dipole antenna. Convergence occurred in 19 segments overall for the half length up to 0.6λ and 21 segments for the half length above 0.6λ and up to 1.05λ. Also plotted in the figure are the results calculated by Harrington[14] for comparison. In his calculation the current is approximated by piecewise-linear function as given by equation (3.47) and 32 segments are used. He observes that pulse function approximation for current gives slower

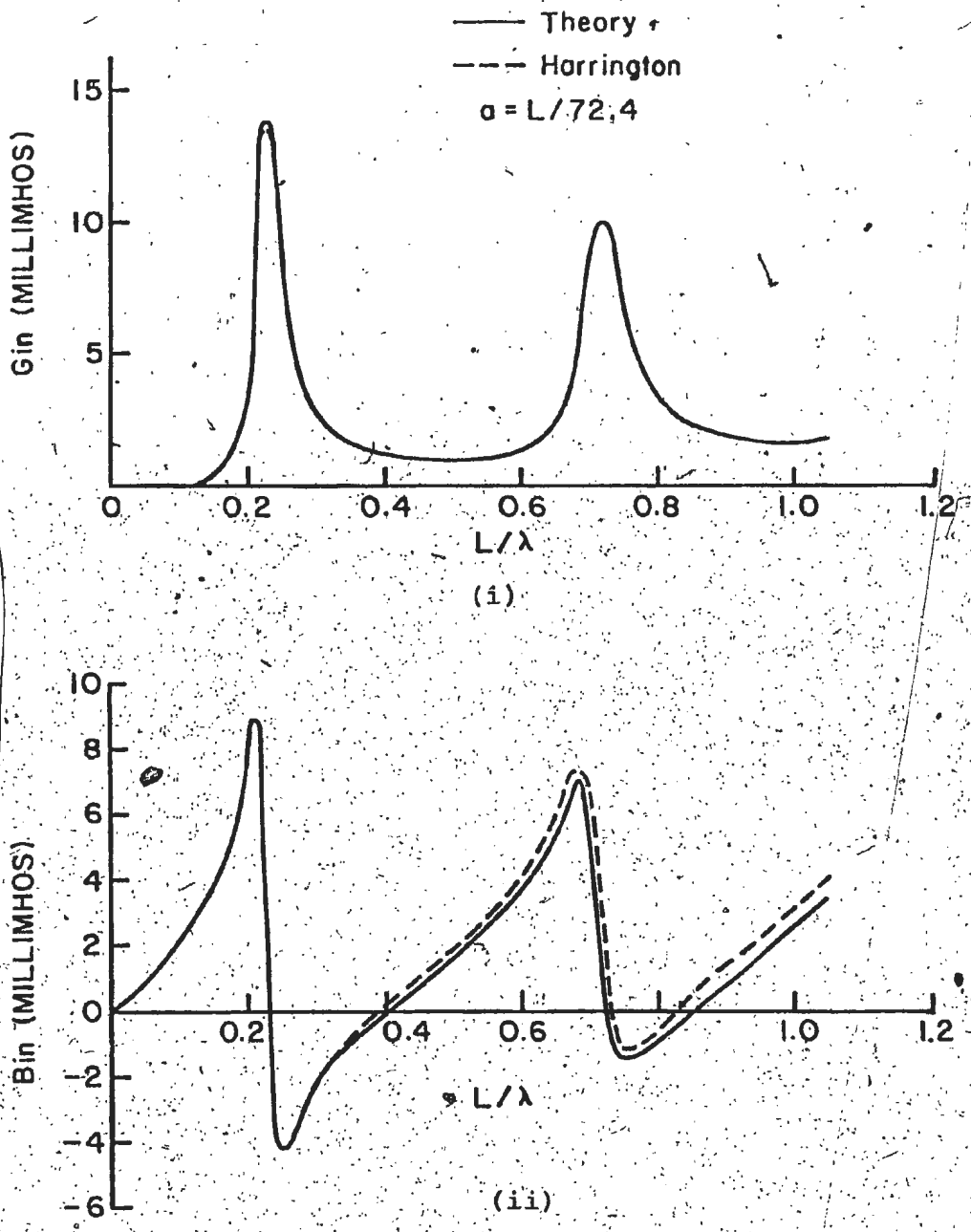

Figure 3.4. Input admittance, (i) conductance (Gin), (ii) susceptance (Bin), for a center-fed dipole as a function of L/λ, radius = L/72.4.

convergence than piecewise-linear approximation. The computed results are in very good agreement with his results except slight difference in susceptance over certain length. This may be because the incident field in his calculation is different than that of a magnetic frill field.

Figure 3.5 shows the current distributions for a three-quarter wave dipole and a one-and-a-quarter wave dipole using 19 segments. The results are compared with measured results by Mack taken from Popovic[22]. It can be seen that calculated results are in close agreement with measured results. The results also closely agree with that found by Popovic using Hallen's equation and polynomial approximation for current.

Finally, the case of singular Green's function is treated. As pointed out earlier, one way to deal with this situation is given in the literature[11]. The other method is to treat the dipole as made up of two wires joined together axially in a straight line. This is a special case of V-antenna when the angle between the two arms is 180°. The V-antenna is discussed in the next chapter. The length of each piece of dipole should be such that the Green's function is not singular. Two examples of this method are given in Figure 3.6. Figure 3.6(i) shows the current distributions for a half wave dipole using 20 segments. Also plotted are the results measured by Mack taken from King[7]. The calculated results are in close agreement with measured

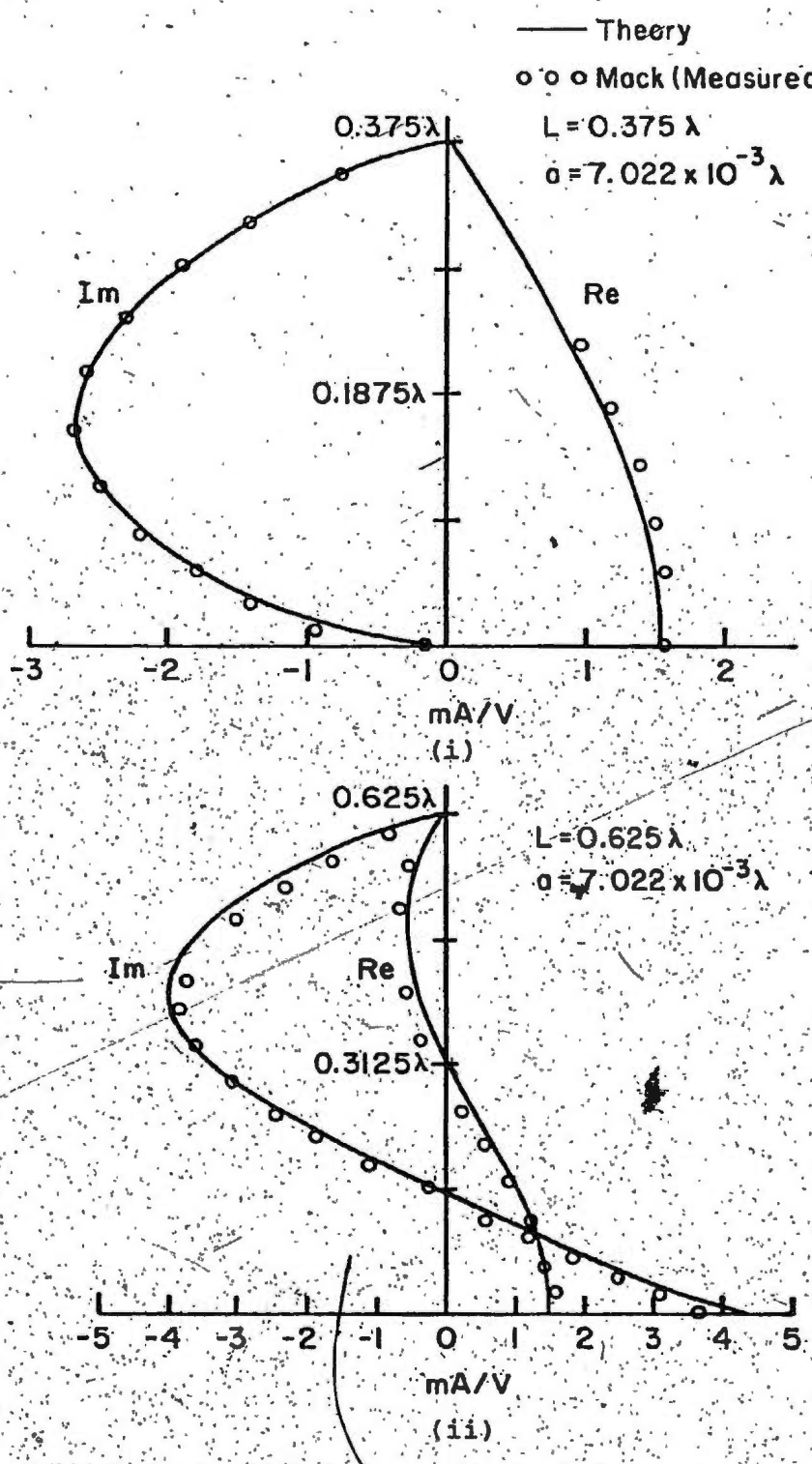

Figure 3.5. Current distributions for a center-fed dipole antenna for (i) three quarter wave dipole, (ii) one and a quarter wave dipole.

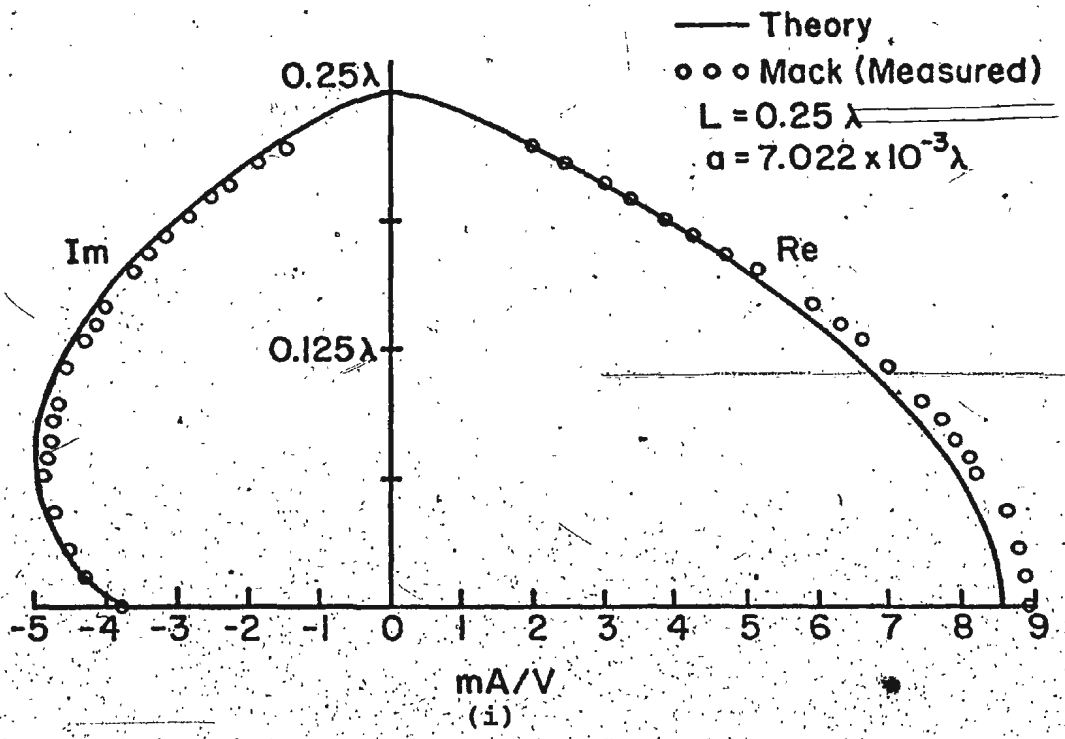

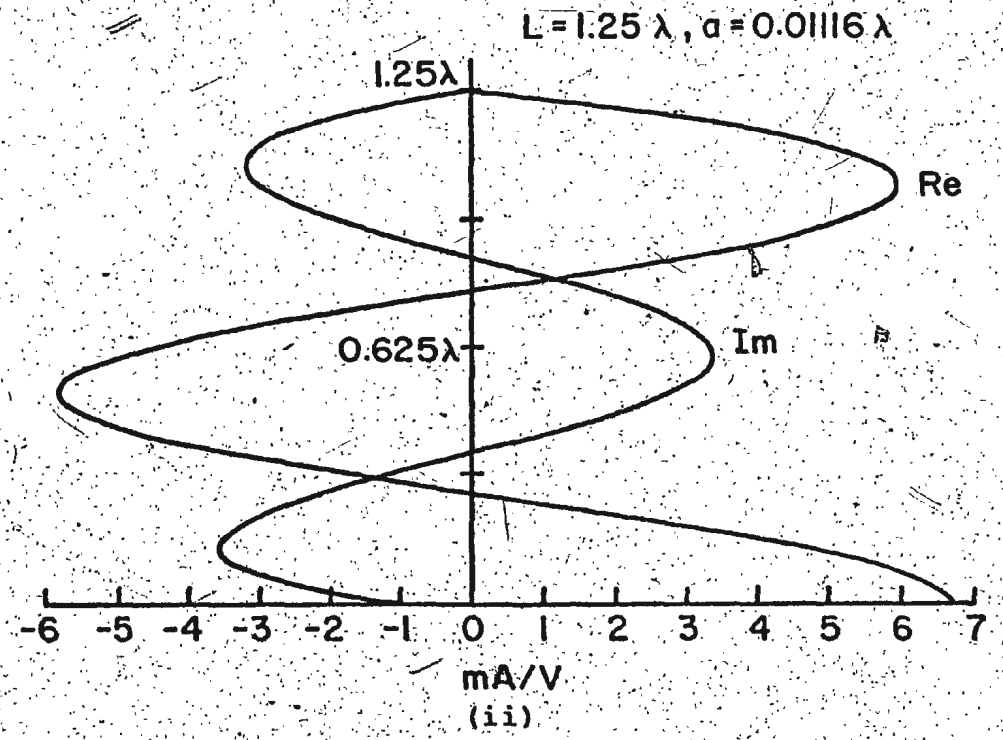

Figure 3.6. Current distributions for a center-fed dipole antenna for (i) half wave dipole, (ii) two and a half wave dipole.

results, in fact better than the results obtained by King using King's three term theory. The second example given in Figure 3.6(ii) shows current distributions for a two-and-a-half wavelength dipole using 26 segments. The results are comparable with that found by Silvester and Chan[20] using Bubnov-Galerkin solution for Pocklington's equation and approximating the current by a fifth order polynomial. The source in the latter is different. A delta-gap generator is used. It should be noted that although the matrix size is small in their method, e.g., order of 10 for the present example, the computation of matrix elements requires evaluation of more complex integrals compared to simple point matching in conjunction with the pulse function method used here.

So far, only the merits of point matching technique in solving the antenna problems have been discussed. This technique has also some drawbacks. The method requires a large number of points. This will give better convergence and sufficient accuracy. This is evident from the results of the examples given earlier. Moreover, point locations are important especially in near field calculations such as input impedence and current distributions. It has been found that more points are required where the slope of the incident field is very steep, e.g., in the near region of the field from a magnetic frill current source for faster convergence. Also matching should not be done at ends, at least about one diameter

away from the ends when using the approximate kernel. This is to avoid the almost singular condition of the radiated field from the end conditions. Of course, higher order techniques like Galerkin's method can be used to solve the integral equation for $E_o(z)$ which will give better convergence but only on losing the simplicity of the point matching technique.

CHAPTER 4

MULTI-ELEMENT STRUCTURES

4.1 Multi-Linear Element Systems

In the last chapter the formulation given in Chapter 2 is successfully applied to simple dipole antennas. In this chapter the technique is extended to multi-linear element systems. For an understanding of the technique of solving such systems, analysis of two such elements is discussed. The method is then easily generalized to n elements.

Consider two linear elements, satisfying the assumptions laid down for a basic linear element in Section (3.1), designated as 1 and 2 and located arbitrarily in space. Let element 1 have a length of $2L_1$ and radius a_1 with its axis coinciding with the z_1 axis and centered at the origin of its cartesian coordinate system $\bar{x}_1$ (x_1, y_1, z_1) or (z_1, ρ_1, ϕ_1) in a cylindrical coordinate system. Similarly, element 2 has a length of $2L_2$ and radius a_2 with its axis coinciding with z_2 axis and centered at the origin of its cartesian coordinate system $\bar{x}_2$ (x_2, y_2, z_2) or (z_2, ρ_2, ϕ_2) in cylindrical coordinates. The geometry of this configuration is shown in Figure 4.1(i). The axial and radial fields from element 1 can be written as

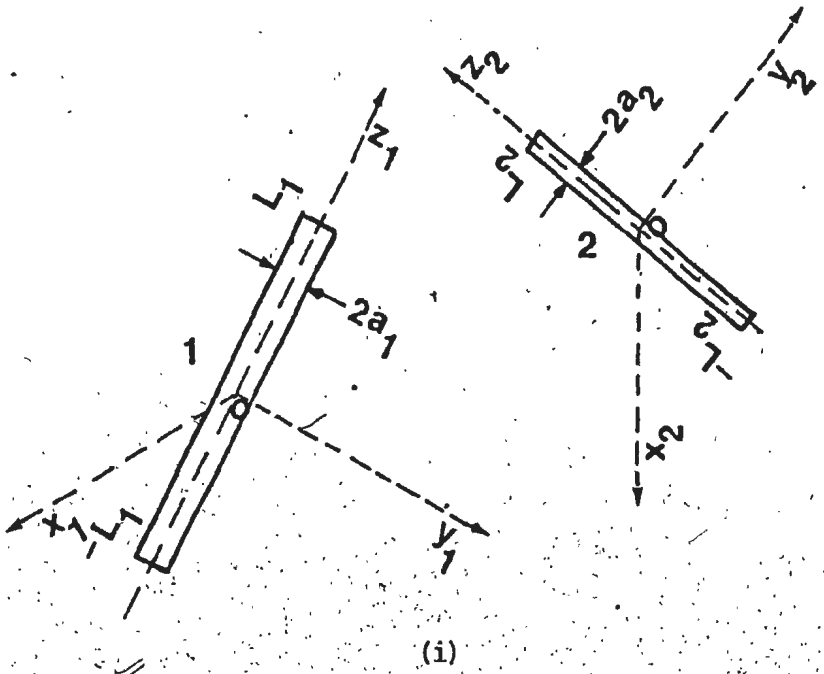

(i)

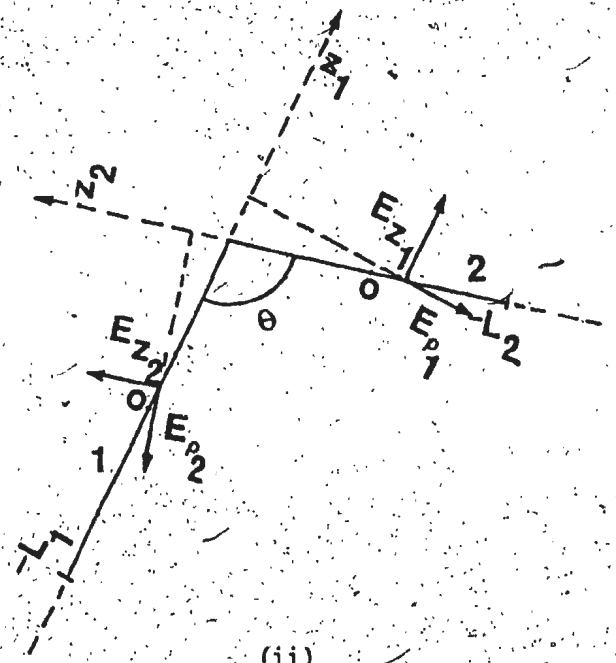

(ii)

Figure 4.1. Two elements of lengths $2L_1$, $2L_2$ and (i) radii a_1, a_2 arbitrarily located in space, (ii) equal radii a axially joined together.

$$E_{z_1}(z_1,\rho_1) = \int_{-L_1}^{L_1} E_{o1}(z_1')\, K_{z_1 c}(z_1/z_1'/\rho_1)\,dz_1'$$

$$+ I_{z_1}(-L_1)K'_{z_1}(z_1+L_1,\rho_1) - I_{z_1}(L_1)K'_{z_1}(z_1-L_1,\rho_1)$$

$$+ b_1 K_{z_1}(z_1+L_1,\rho_1) - c_1 K_{z_1}(z_1-L_1,\rho_1) \qquad (4.1)$$

$$E_{\rho_1}(z_1,\rho_1) = -[\int_{-L_1}^{L_1} E_{o1}(z_1')\, K_{\rho_1 c}(z_1/z_1'/\rho_1)\,dz_1'$$

$$+ I_{z_1}(-L_1)K'_{\rho_1}(z_1+L_1,\rho_1) - I_{z_1}(L_1)K'_{\rho_1}(z_1-L_1,\rho_1)$$

$$+ b_1 K_{\rho_1}(z_1+L_1,\rho_1) - c_1 K_{\rho_1}(z_1-L_1,\rho_1)] \qquad (4.2)$$

where the primes denote differentiation with respect to z_1. $K_{z_1 c}$ and $K_{\rho_1 c}$ are given by equations (3.19) and (3.20) with L and a replaced by L_1 and a_1, and (z,ρ) by (z_1,ρ_1). b_1 and c_1 are given respectively by equations (3.21) and (3.22) by putting L_1 for L with end currents $I_{z_1}(-L_1)$ and $I_{z_1}(L_1)$. K_{z_1} and K_{ρ_1} are given as before by equations (3.6) and (3.7) with necessary change a_1 for a. E_{o1} is given by equation (3.10).

The equation for the current in this case can be written from equation (3.15) as

$$I_{z_1}(z_1) = I_{z_1}(-L_1)\frac{\sin[k(L_1-z_1)]}{\sin(2kL_1)} + I_{z_1}(L_1)\frac{\sin[k(L_1+z_1)]}{\sin(2kL_1)}$$

$$+ \int_{-L_1}^{L_1} G_1(z_1/z_1')\, E_{o1}(z_1')\,dz_1' \qquad (4.3)$$

where $G_1(z_1/z_1')$ is given by equation (3.16) with L replaced by L_1.

For simplicity in computations again an approximate kernel $K_{z_1 a}$ will be used instead of the actual kernel K_{z_1} [4,19,20]. This replaces $K_{z_1}(z_1,\rho_1)$ by

$$K_{z_1 a}(z_1,\rho_1) = \frac{\exp[-jk(z_1^2+\rho_1^2+a_1^2)]^{\frac{1}{2}}}{j4\pi\omega\varepsilon(z_1^2+\rho_1^2+a_1^2)^{\frac{1}{2}}} \qquad (4.4)$$

For calculating scattered field ρ_1 equals zero and thus

$$K_{z_1 a}(z_1,0) = \frac{\exp[-jk(z_1^2+a_1^2)]^{\frac{1}{2}}}{j4\pi\omega\varepsilon(z_1^2+a_1^2)^{\frac{1}{2}}} \qquad (4.5)$$

Similarly, $K_{\rho_1}(z_1,\rho_1)$ is replaced by its approximation given by

$$K_{\rho_1 a}(z_1,\rho_1) = \frac{z_1\rho_1}{\rho_1^2+a_1^2}\, K_{z_1 a}(z_1,\rho_1) \qquad (4.6)$$

It can be seen that equation (4.6) for $K_{\rho_1 a}$ is obtained from equation (4.4) for $K_{z_1 a}$ on a similar basis as the exact kernel K_ρ given by (3.7) is obtained from equation (3.6) for the exact kernel K_z in Appendix (B.2) when K_z

is replaced by $K_{z_1 a}$. For the above choice of approximate kernels, $K_{z_1 c}$ and $K_{\rho_1 c}$ in equations (4.1) and (4.2) would be replaced by their approximations $K_{z_1 ac}$ and $K_{\rho_1 ac}$ respectively, where $K_{z_1 ac}$ and $K_{\rho_1 ac}$ are given from the equations (3.19) and (3.20) for K_{zc} and $K_{\rho c}$ with the change that actual kernels K_{z_1} and K_{ρ_1} are replaced by the approximate kernels $K_{z_1 a}$ and $K_{\rho_1 a}$, respectively, as in equations (C.27) and (C.29).

For element 2 the equations for field components and current are not given here. They can be written directly from the equations given for element 1 by just changing the subscript from 1 to 2 in the various terms. The angular component of fields ($E\phi$) for both elements are zero as shown earlier in the case of the basic linear element in Appendix (B.3).

Since the elements are perfect conductors they cannot support any tangential component of the electrical field. As such, the sum of scattered field and tangential incident fields from all other sources will be zero. Mathematically the sum of fields for both elements can be written with reference to Figure 4.1(i) in the form of coupled equations as

$$E^s_{z_1}(z_1,0) + \hat{z}_1 E_{z_2}(z_2,\rho_2) + \hat{z}_1 E_{\rho 2}(z_2,\rho_2) = -E^i_{z_1}(z_1,0) \qquad (4.7)$$

$$\hat{z}_2 E_{z_1}(z_1,\rho_1) + \hat{z}_2 E_{\rho_1}(z_1,\rho_1) + E^s_{z_2}(z_2,0) = -E^i_{z_2}(z_2,0) \qquad (4.8)$$

where

$E^s_{z_1}(z_1,0)$ is the scattered field of element 1 at any observation point on its axis z_1 between $-L_1$ and L_1.

$E_{z_2}(z_2,\rho_2)$ and $E_{\rho_2}(z_2,\rho_2)$ are respectively the axial and radial fields radiated from element 2 at same observation point on z_1 with reference to its coordinate axis $\bar{x}_2$.

$E^s_{z_2}(z_2,0)$ is the scattered field of element 2 at any observation point on its axis z_2 between $-L_2$ and L_2.

$E_{z_1}(z_1,\rho_1)$ and $E_{\rho_1}(z_1,\rho_1)$ are respectively the axial and radial fields from element 1 evaluated at same observation point on z_2 with reference to its own coordinate axis $\bar{x}_1$.

$E^i_{z_1}$ and $E^i_{z_2}$ are the incident fields on element 1 and 2 respectively along their axes from some external source or sources.

$\hat{z}_1$ and $\hat{z}_2$ refer to the projections of the associated fields or their components on z_1 and z_2 axes, respectively.

Now two different conditions, namely the condition of free ends and the condition of joints will be considered.

4.1.1 Treatment of Free Ends Condition

This condition is usually encountered in antenna arrays, e.g., Yagi-uda array. Under this condition the end currents are zero. Therefore, the coupled integral equations (4.7) and (4.8) can be expanded with the help of equations (4.1) and (4.2) as ,

$$\int_{-L_1}^{L_1} E_{o1}(z_1')K_{z_1ac}(z_1/z_1'/0)\,dz_1' + \int_{-L_2}^{L_2} E_{o2}(z_2')\,\{\hat{z}_1 K_{z_2ac}(z_2/z_2'/\rho_2)$$

$$- \hat{z}_1 K_{\rho_2 ac}(z_2/z_2'/\rho_2)\}\,dz_2' = -E^i_{z_1}(z_1,0) \qquad (4.9)$$

and

$$\int_{-L_1}^{L_1} E_{o1}(z_1')\{\hat{z}_2 K_{z_1ac}(z_1/z_1'/\rho_1) - \hat{z}_2 K_{\rho_1 ac}(z_1/z_1'/\rho_1)\}\,dz_1'$$

$$+\int_{-L_2}^{L_2} E_{o2}(z_2')K_{z_2ac}(z_2/z_2'/0)\,dz_2' = -E^i_{z_2}(z_2,0) \qquad (4.10)$$

where z_2 and ρ_2 in equation (4.9) are determined in terms of coordinates of any observation point on z_1 with respect to $\bar{x}_2$. Similarly, z_1 and ρ_1 in equation (4.10) are determined in terms of coordinates of any observation on z_2 with respect to $\bar{x}_1$. For the given incident fields E^i_z and $E^i_{z_2}$ the above set of two simultaneous integral equations can be solved for $E_{o1}(z_1')$ and $E_{o2}(z_2')$ by using any standard technique such as discussed earlier for the case of the dipole antenna. From the solution for $E_{o1}(z_1')$, the current distributions for element 1 can be determined with the help of equation (4.3). Similarly, from the solution for $E_{o2}(z_2')$, the current distributions for element 2 may be determined. If there are n such elements this technique can easily be extended resulting in n simultaneous integral equations. Further, these n equations can be solved for n unknown $E_o(z_n')$'s and the current distributions for all n elements

may be determined.

4.1.2 Treatment of Joints

Joints between the various elements are very common in a multi-wires antenna. A few good examples are V, rhombic and top-loaded antennas. In treating joints the following assumptions are made, parallel to that of other workers, in addition to those already made for a linear element.

(i) All joints are axial without occupying any space and do not give rise to off axial currents.

(ii) All the elements joining together have equal radii.

It is shown in Appendix (C.1) that for n elements joining together, when Kirchoff's current law is applied at the junction and using the approximate kernels, higher order fields, i.e., the terms with derivatives in equations (4.1) and (4.2) cancel with the result that the following equations may be used for the radiated axial and radial fields:

$$E_{z_1}(z_1,\rho_1) = \int_{-L_1}^{L_1} E_{o1}(z_1')K_{z_1ac}(z_1/z_1'/\rho_1)dz_1'$$

$$+ b_1K_{z_1a}(z_1+L_1,\rho_1) - c_1K_{z_1a}(z_1-L_1,\rho_1) \qquad (4.11)$$

$$E_{\rho_1}(z_1,\rho_1) = -\left[\int_{-L_1}^{L_1} E_{o1}(z_1')K_{\rho_1ac}(z_1/z_1'/\rho_1)dz_1'\right.$$

$$\left. + d_1K_{\rho_1a}(z_1+L_1,\rho_1) - e_1K_{\rho_1a}(z_1-L_1,\rho_1)\right] \qquad (4.12)$$

where

$$d_1 = b_1 - j\, I_{z_1}(-L_1)\, \frac{k}{z_1+L_1}\, r(z_1+L_1, \rho_1) \qquad (4.13)$$

$$e_1 = c_1 - j\, I_{z_1}(L_1)\, \frac{k}{z_1-L_1}\, r(z_1-L_1, \rho_1) \qquad (4.14)$$

where r is defined in general as

$$r(z,\rho) = (z^2+\rho^2+a^2)^{\frac{1}{2}} \qquad (4.15)$$

If it is assumed that all joining elements have common points of contact the higher order fields should cancel when the exact kernels are used. Physically the existence of higher order fields implies a discontinuous current or a current which does not obey Kirchoff's current law at the junction. Of course, such a current source cannot exist.

Consider the two elements 1 and 2 joined together at their ends (L_1, L_2) as shown in Figure 4.1(ii). For simplicity, only their axes are shown in figure. The angle between their axes is θ. Since their other ends $(-L_1, -L_2)$ are free, $I_{z_1}(-L_1)$ and $I_{z_2}(-L_2)$ vanish. For such a case equations (4.7) and (4.8) can be expanded with the help of equations (4.11) and (4.12) and Figure 4.1(ii) as shown in Appendix (C.2). For a known incident field, the resulting coupled integral equations (C.21) and (C.22) in conjunction with Kirchoff's current law equation (C.36) for the junction may be solved for $E_{o1}(z')$, $E_{oz}(z')$ and end currents $I_{z_1}(L_1)$, $I_{z_2}(L_2)$ by any suitable technique. From the solutions

current distributions for element 1 may be determined from equation (4.3) and similarly for element 2.

If there are n linear elements, joined or separated or both, in space forming a multi-elements structure, these equations can easily be generalized. This will give n simultaneous integral equations with n Kirchoff's current law equations where m is number of joints in the structure. These equations may be solved for unknowns, for a given incident field, and the current distributions for all elements and thus input impedence determined. The case of unequal radii of elements joining together is not considered since this is not a good model for practical multi-wires antennas.

4.2 Numerical Results and Comparison

As an example for the two element structure a V-antenna[15] is solved using equations (C.21), (C.22), (C.36), and (4.3). For multi-element structures a top loaded antenna[16] is solved using a generalization of these equations. In both cases input impedence and current distributions are determined. The source is again a magnetic frill current. The numerical technique used for solution is point matching in conjunction with pulse functions. This is similar to that used for the case of dipole antenna earlier. This technique is again selected because the advantages already mentioned in Section (3.2.7) of the dipole antenna. Also, as pointed

out earlier in the same section, the integral of the composite kernel $K_{\rho_{ac}}$ for the radial field is available in closed form for such a choice as shown in Appendix (C.3).

4.2.1 V-Antenna

Figure 4.2(i) shows a monopole protruding from an infinite and perfect ground plane. It is fed at its base. The monopole with its image is modeled as two symmetrical linear elements joined together forming a V-antenna. Figure 4.2(ii) shows the input admittance of a quarter wave monopole as a function of angle of inclination from ground plane normal (α). Also plotted in the figure are the results measured by Lekhyananda taken from Jones[23] for comparison. It can be seen that there is a good agreement between the two results for α up to 50°, and less agreement for α greater than that. The probable reason for this discrepancy is that at higher α, the angle between the two elements (θ) in the model is less. This means that the overlap between the two elements is more at the joint, giving significant off axial current. This departs from the assumption of an ideal joint. Also, the use of approximate kernels may produce some discrepancies in the results. Figure 4.3 shows again the input admittance of the monopole in another case. In this Y_{in} is given as a function of length for a fixed α of 30°. The results are compared again with the measured results of Lekhyananda. Again the agreement is good. In

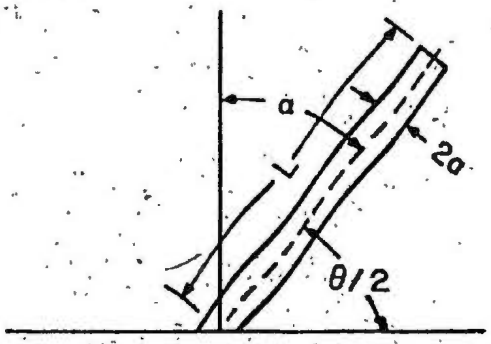

(i)

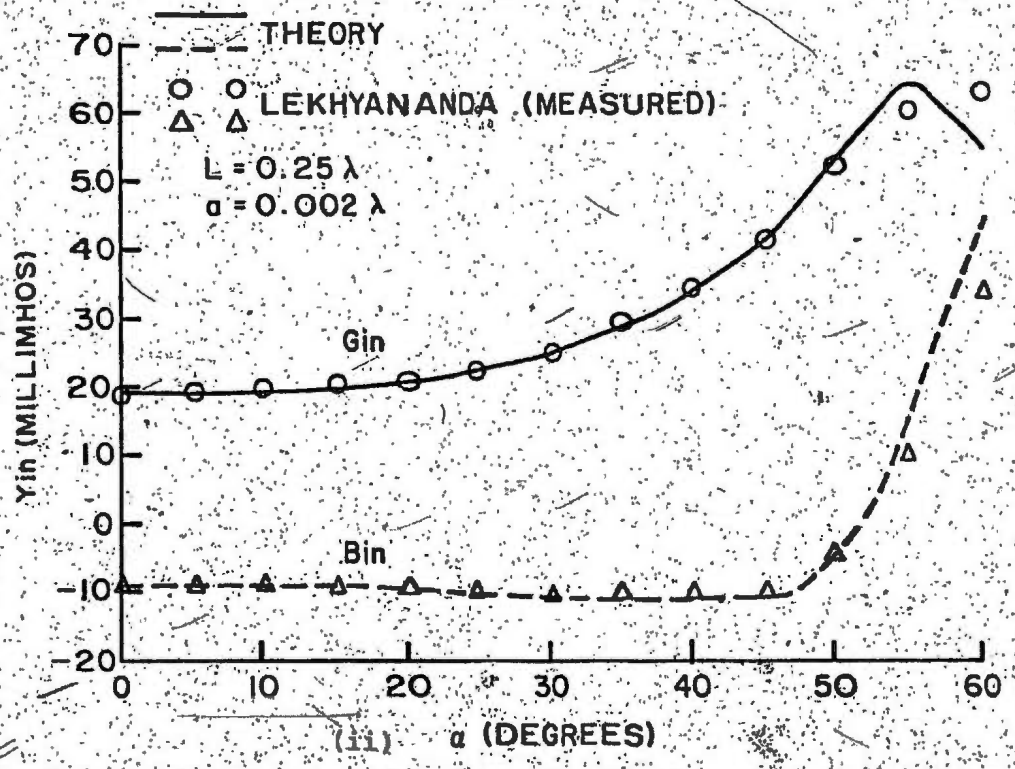

(ii)

Figure 4.2. (i). Monopole inclined at an angle α from ground plane normal.
(ii). Input admittance of a base fed quarter wave monopole as a function of angle α.

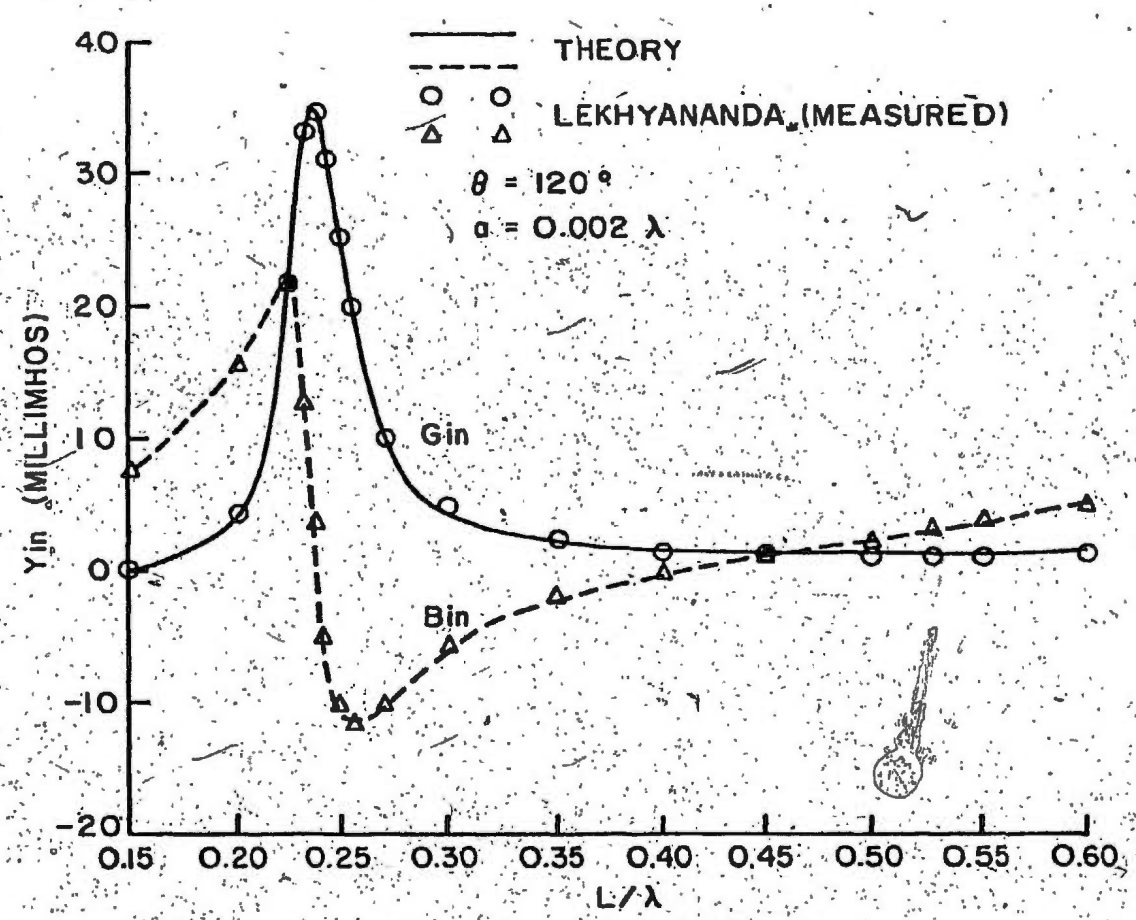

Figure 4.3. Input admittance of a base fed monopole as a function of length L for a = 30°.

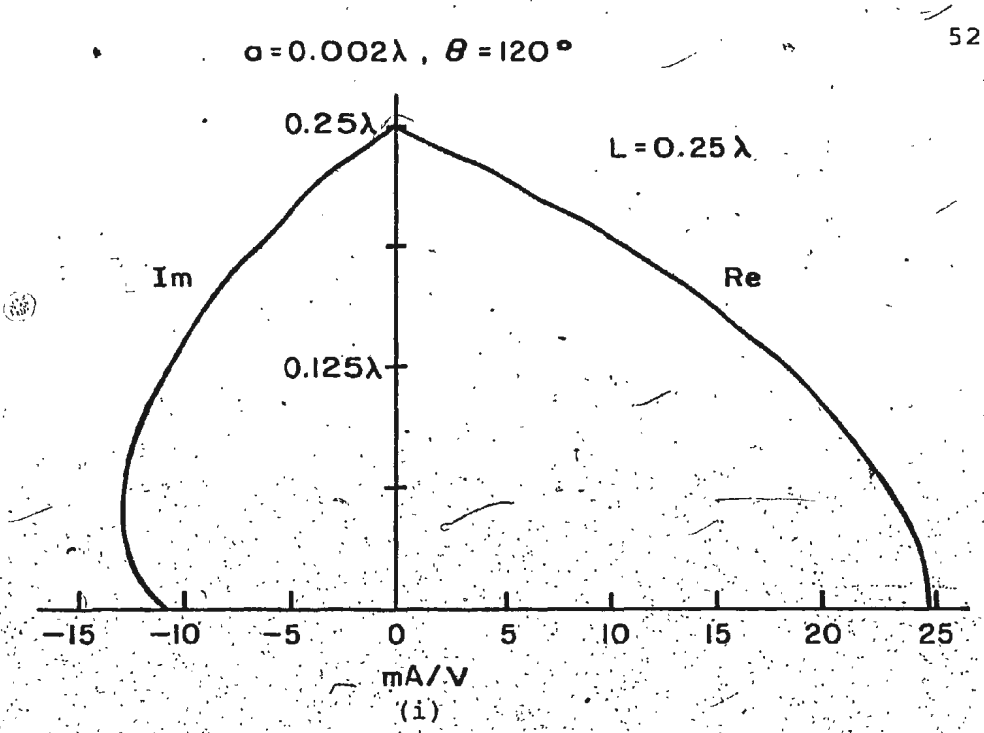

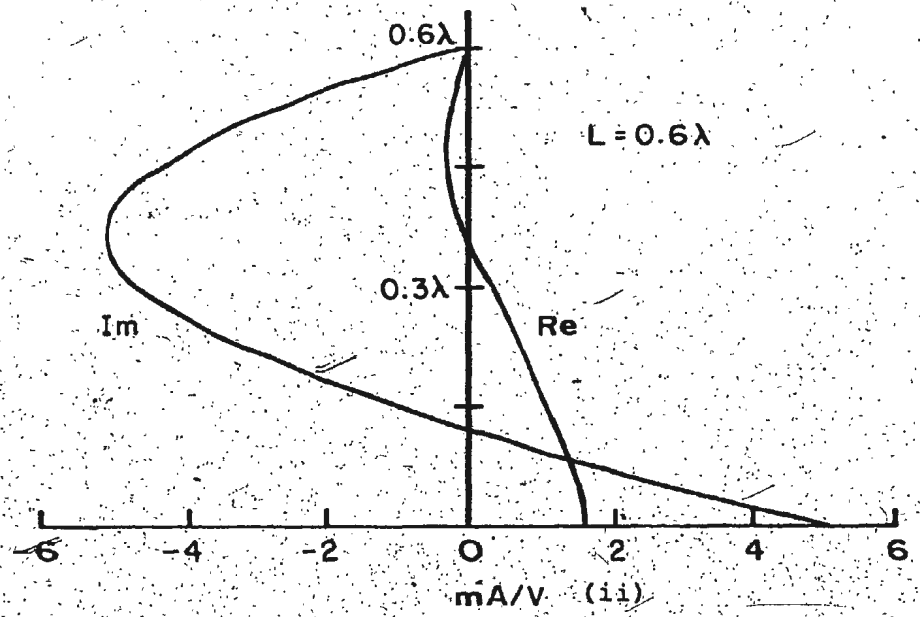

Figure 4.4. Current distributions for a base fed monopole for $\alpha = 30^{\circ}$ and for (i) $L=0.25\lambda$, (ii) $L=0.6\lambda$.

both cases the results are similar to that calculated by Jones. Current distributions are also calculated for the monopole for $\alpha = 30^{\circ}$. The results are plotted in Figure 4.4(i) for quarter wave monopole and in Figure 4.4(ii) for the length of 0.6λ. In all the results the monopole was divided into 10 segments.

Next, the current distributions for a symmetrical center fed V-antenna of Figure 4.5(i) are calculated for $\theta = 90^{\circ}$ using 11 segments per arm for the cases shown. The results for half wave V-antenna are given in Figure 4.5(ii). Figure 4.6 includes the results for half length (L) of 0.2λ, 0.4λ, and 0.6λ. The agreement of the results is good, in general, when compared with the results of Jones[23]. Little discrepancies in the results for lengths of 0.4λ and 0.6λ may be due to the different sources used for excitation. A delta-gap generator is used by Jones and the numerical technique used is Galerkin type moment method in conjunction with piecewise sinusoidal expansion of current. The number of segments used are only 5 per arm but the integrations involved are much more complex compared to simple point matching technique in conjunction with pulse functions. A special case of V-antenna is a linear dipole ($\theta = 180^{\circ}$). For this case also the current distributions for two different lengths have been determined and are shown in Figure 3.6. The reference of this is already given in the section (3.2.7) of the dipole.

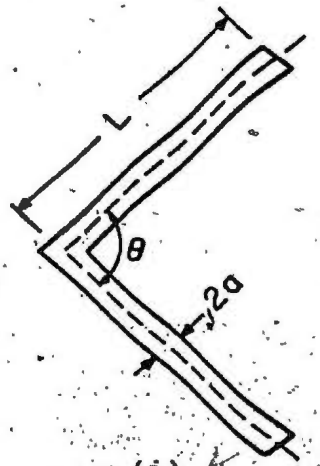

(i)

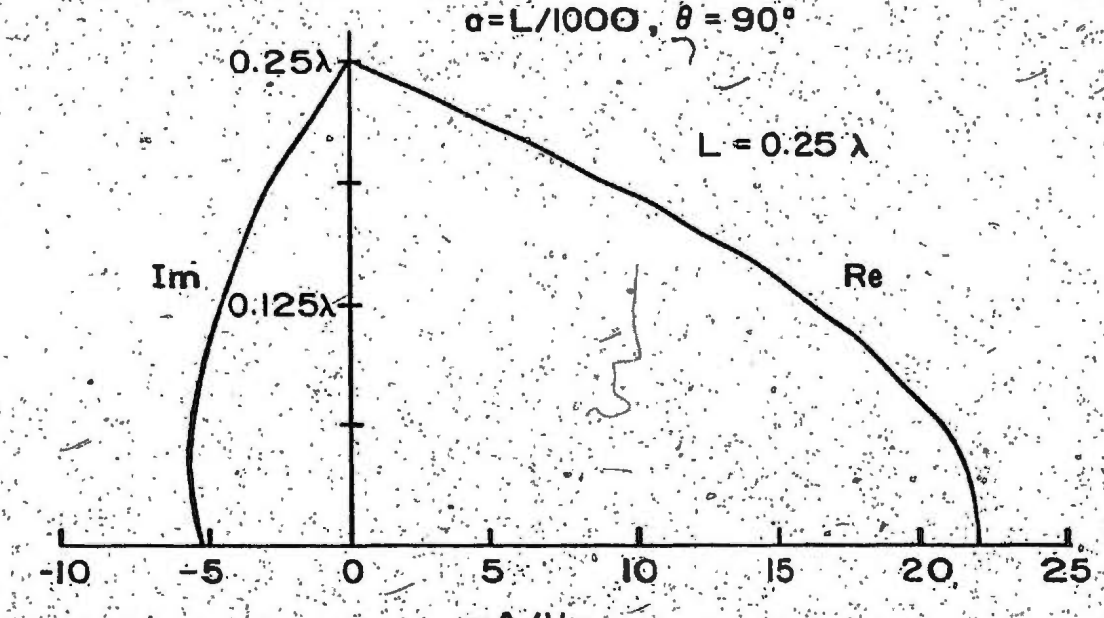

(ii)

Figure 4.5. (i). Symmetrical V-antenna.
(ii). Current distributions for a half wave symmetrical center-fed V-antenna for $\theta = 90^{\circ}$.

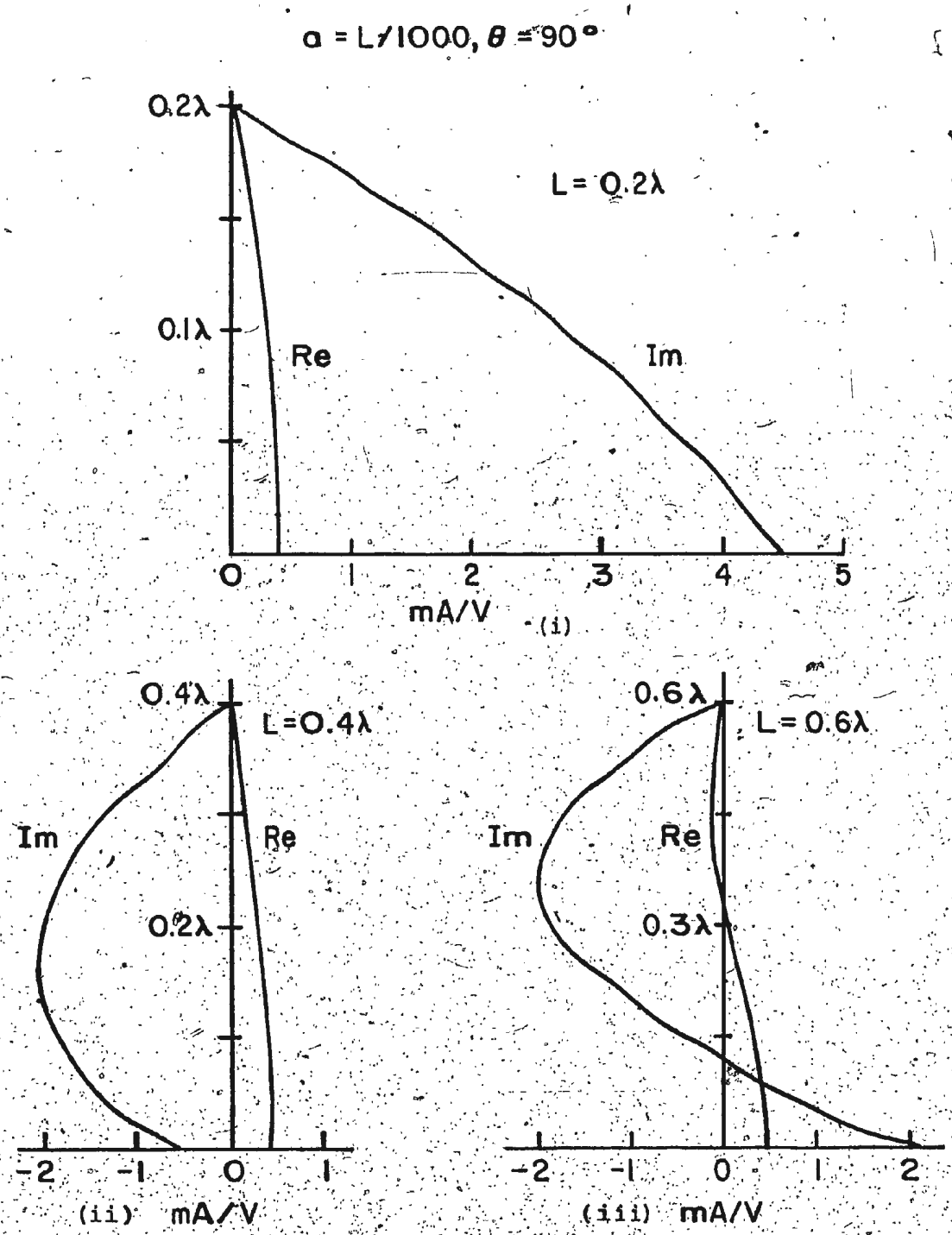

Figure 4.6. Current distributions for a symmetrical center-fed V-antenna for $\theta = 90°$ and for (i) $L=0.2\lambda$, (ii) $L=0.4\lambda$, (iii) $L=0.6\lambda$.

4.2.2 Top Loaded Antenna

A symmetrical two element top loaded antenna protruding from an infinite and perfect ground plane is shown in Figure 4.7(i). The antenna is fed at its base. It, together with its image, is modelled by six linear elements, three for the antenna and three for its image. The input impedence of a T-antenna with $k(H+L) = \pi/2$ and $\theta = 90^{\circ}$ is calculated using 10 segments from center to either of the top end. The result as a function of kH is shown in Figure 4.7(ii). Also plotted in the figure are experimental values given by Simpson for the same structure[24,20]. It may be seen that the agreement between theory and experimental values is good. It is of interest to note that Simpson uses the generalized Hallen's equation, 25 segments, and point matching to obtain theoretical curves like Figure 4.7(ii).

Figure 4.8 shows the computed current distributions for the same structure for two different angles $\theta = 90^{\circ}$ and $\theta = 45^{\circ}$ with $H=L=\lambda/8$ using same number of segments. The results are compared with measured values given by Simpson[20]. Again the agreement is good; in fact, better than Simpson's theoretical results[20]. Discrepancies between theoretical and measured values in Figures 4.7 and 4.8 may be attributed to the use of approximate kernels and current distributions different from that assumed at the junction. The results of both the figures are similar to those found by Silvester and

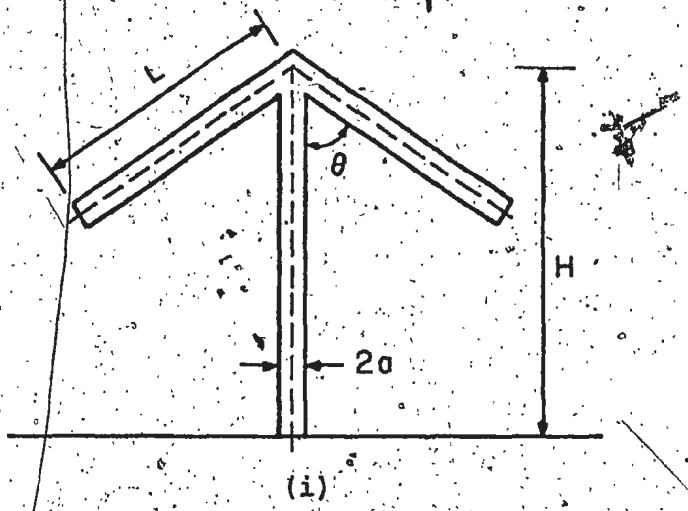

(i)

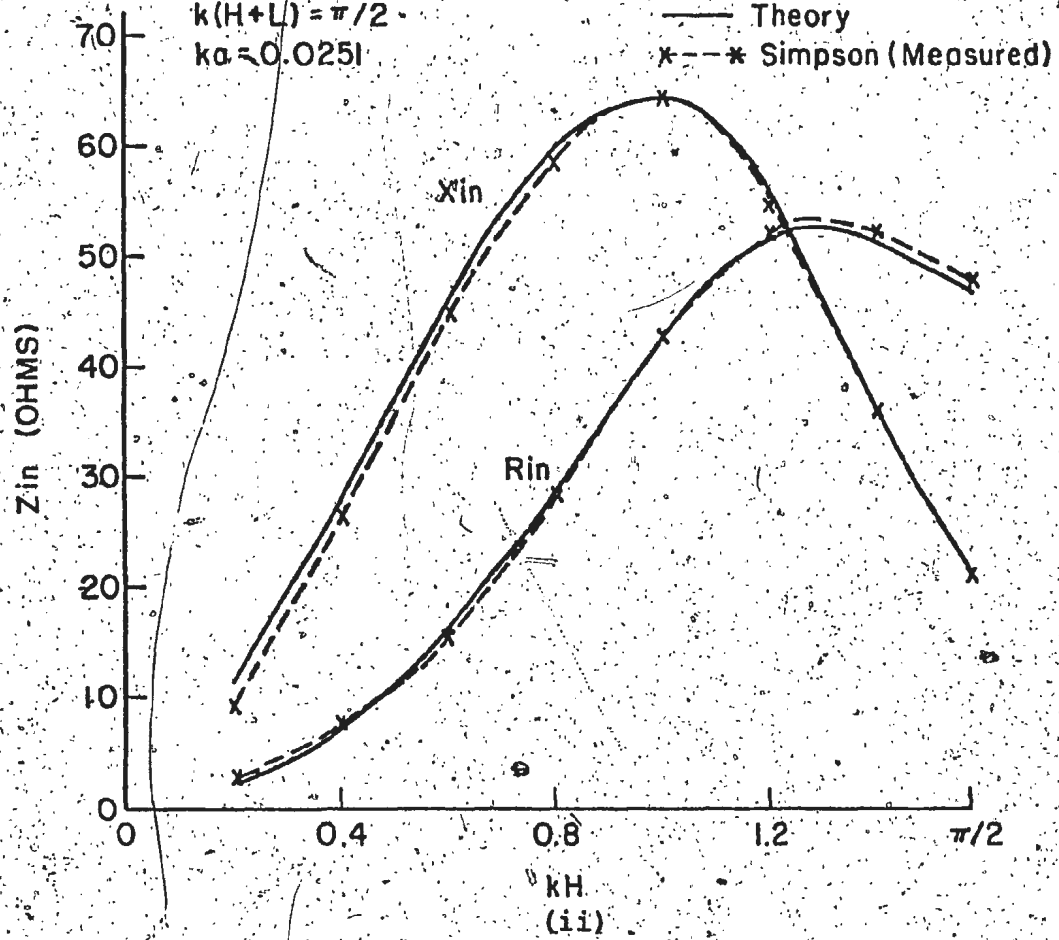

(ii)

Figure 4.7.(i). Symmetrical two element top loaded antenna.
(ii). Input impedence of a base fed symmetrical $T(\theta=90^{o})$ antenna as a function of kH.

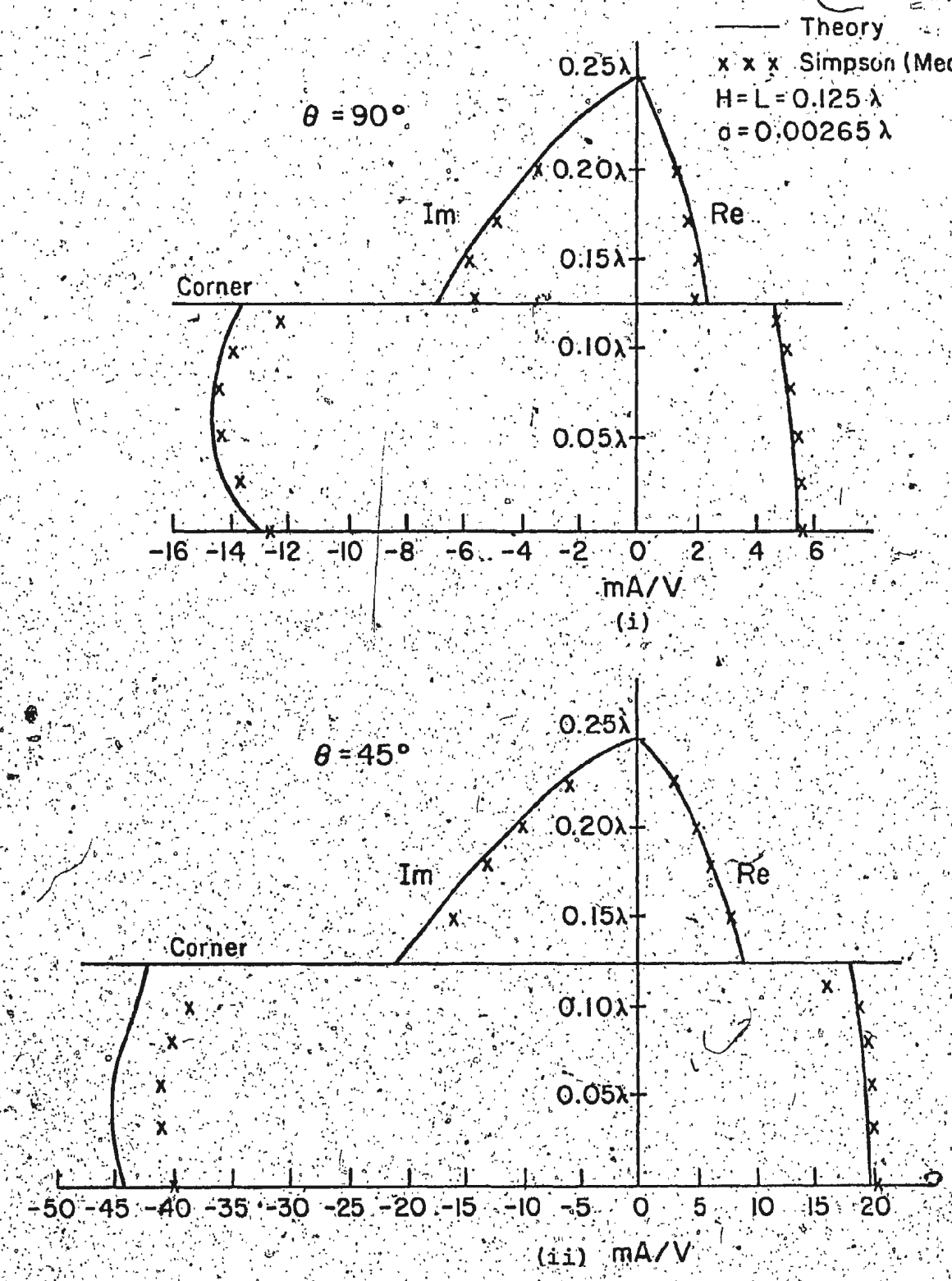

Figure 4.8. Current distributions for a symmetrical two element top loaded base fed antenna for (i) $\theta=90^{o}$, (ii) $\theta=45^{o}$.

Chan using Bubnov-Galerkin solution for Pocklington's integral equation and approximating the current by a polynomial. Again the evaluation of matrix elements is complex although the size of the matrix is small.

CHAPTER 5

CONCLUSIONS

The method of analysis of linear antenna systems proposed in this thesis eliminates the need of imposing boundary conditions on the solution of an integral operator. This is achieved by first inverting a commuting differential operator which satisfies the boundary conditions. This method is particularly effective since the solution of the differential equation can be written in closed form for a linear element as in equation (3.15).

The computed results based on the proposed method closely agree with those found by other investigators both theoretically and by measurement. It has been shown, for the examples given, that the method has certain numerical advantages over the classical Pocklington's formulation. Numerical results based on the proposed method show a rate of convergence far superior to that of Pocklington's formulation when point matching technique in conjunction with pulse functions is used to solve the integral equation in both. The rates are comparable when entire domain cosine bases are used instead of pulse functions for solving Pocklington's equation. Also, the method proposed here has the flexibility of Pocklington's equation when compared to Hallen's equation.

Although in this thesis attention is confined to the use of a point matching technique in conjunction with pulse functions as a method of solution of the integral equation based on the proposed method, it is not implied that the proposed method using this numerical technique is superior from the point of view of convergence to some of the variational techniques proposed by other workers. However, these variational techniques are not so simple to apply as point matching. Examples of these are the papers of Jones[23], and Silvester and Chan[20], who have analyzed respectively the V-antenna of Section (4.2.1) and the top loaded antenna of Section (4.2.2). These variational techniques can of course be used for solution in the proposed method and it is hoped to make this the subject of a further investigation.

Finally, the results of Chapter 2 are quite general. Equation (2.19) clearly demonstrates the relationship between antenna problems and mechanical vibrations, the right-hand side providing a forcing function for the differential equation $T(\bar{J}_s)$. In the case of a dipole, the solution (3.35) is merely that of a well known vibrating string with $E_o(z)$ providing a driving function. Although in this thesis the utilization of the general formulation given in Chapter 2 is restricted to linear antenna systems, this can very well be applied to other antenna systems, especially where the differential operator is invertible in closed form.

REFERENCES

1. Pocklington, H.C., "Electrical Oscillations in Wires," Proc. Camb. Phil. Soc., 1897, Vol. 9, pp. 324-332.

2. Hallén, E., "Theoretical Investigation into the Transmitting and Receiving Qualities of Antennae," Nova Acta Soc. Sci. Upsal., 1938, Ser. IV, 11, pp. 1-44.

3. Mie, K.K., "On the Integral Equations of Thin Wire Antennas," IEEE Trans. on Ant. and Prop., 1965, Vol. AP-13, No. 3, pp. 374-378.

4. Thiele, G.A., "Wire Antennas," in, "Computer Techniques for Electromagnetics," Pergamon Press, 1973, pp. 7-95.

5. King, R.W.P., "Theory of Linear Antennas," Harvard Univ. Press, Cambridge, Mass., 1956.

6. King, R.W.P., and Harrison, C.W., "Antennas and Waves: A Modern Approach," M.I.T. Press, Cambridge, Mass., 1969.

7. King, R.W.P., "Cylindrical Antennas and Arrays," in, "Antenna Theory," Part I, McGraw-Hill, 1969, pp. 352-420.

8. King, R.W.P., "The Linear Antenna - Eighty Years of Progress," Proc. IEEE, 1967, Vol. 55, No. 1, pp. 2-16.

9. Walsh, J., "Solution of Currents on Linear Antennas," Electron. Lett., 1976, Vol. 12, No. 12, pp. 308-309.

10. Walsh, J., "On the Solution of Antenna Currents," Digest IEEE AP-S International Symposium, Amherst, Mass., Oct. 1976, pp. 197-200.

11. Walsh, J., "Solution of Currents on Linear Antennas: Eigenfunctions and Resonance," Electron. Lett., 1977, Vol. 13, No. 1, pp. 17-19.

12. Gel'fand, I.M., and Shilov, G.E., "Generalized Functions," Vol. 1, Academic Press, 1964.

13. Delves, L.M., and Walsh, J., "Numerical Solution of Integral Equations," Oxford Press, 1974.

14. Harrington, R.F., "Matrix Methods for Field Problems," Proc. IEEE, 1967, Vol. 55, No. 2, pp. 136-149.

15. Walsh, J., and Srivastava, S.K., "A Method of Analysis for Thin, Tubular, Linear Antennas," Digest IEEE AP-S International Symposium, Stanford, Calif., June 1977, pp. 477-480; also in, Proc. URSI Electromagnetic Wave Theory Symposium, Stanford, Calif., June 1977, pp. 115-118.

16. Walsh, J., and Srivastava, S.K., "A Method of Analysis of Linear Antenna Systems," submitted to Proc. IEE.

17. Jordan, E.C., and Balmain, K.G., "Electromagnetic Waves and Radiating Systems," Prentice Hall, 1968.

18. Tsai, L.L., "Near and Far Fields of a Magnetic Frill Current," Digest URSI Spring Meeting, 1970.

19. Richmond, J.H., "A Wire-Grid Model for Scattering by Conducting Bodies," IEEE Trans. on Ant. and Prop., 1966, Vol. AP-14, No. 6, pp. 782-786.

20. Silvester, P., and Chan, K.K., "Analysis of Antenna Structures Assembled from Arbitrarily Located Straight Wires," Proc. IEE, 1973, Vol. 120, No. 1, pp. 21-26.

21. Rumsey, V.H., "Reaction Concept in Electromagnetic Theory," Physical Review, 1954, Vol. 94, No. 6, pp. 1483-1491.

22. Popovic, B.D., "Polynomial Approximation of Current Along Thin Symmetrical Cylindrical Dipoles," Proc. IEE, 1970, Vol. 117, No. 5, pp. 873-878.

23. Jones, J.E., "Analysis of the Symmetric Centre-Fed V-Dipole Antenna," IEEE Trans. on Ant. and Prop., 1976, Vol. AP-24, No. 3, pp. 316-322.

24. Simpson, T.L., "The Theory of Top-Loaded Antennas: Integral Equations for the Currents," IEEE Trans. on Ant. and Prop., 1971, Vol. AP-19, No. 2, pp. 186-190.

APPENDIX A

A.1 Helmholtz Equation

In a steady state sinusoidal case with radian frequency ω, Maxwell's four field equations in phasor form, for the infinite, nonconductive, homogeneous, isotropic medium with permeability μ and permittivity ϵ having a current source $\bar{J}(\bar{x})$, are given as[17],

$$\nabla \times \bar{H}(\bar{x}) = j\omega\epsilon\bar{E}(\bar{x}) + \bar{J}(\bar{x}) \qquad (A.1)$$

$$\nabla \times \bar{E}(\bar{x}) = -j\omega\mu\bar{H}(\bar{x}) \qquad (A.2)$$

$$\nabla \cdot \bar{E}(\bar{x}) = \frac{\rho_c}{\epsilon} \qquad (A.3)$$

$$\nabla \cdot \bar{H}(\bar{x}) = 0 \qquad (A.4)$$

Contained in the above is the equation of continuity, given as

$$\nabla \cdot \bar{J}(\bar{x}) = -j\omega\rho_c \qquad (A.5)$$

where H = magnetic field strength

E = electrical field strength or intensity

ρ_c = charge density

J = current density of the source

Equation (A.4) is satisfied if $\bar{H}$ is written as the curl of some vector, which gives the following definition of the vector potential $\bar{A}$.

$$\nabla \times \bar{A}(\bar{x}) = \mu\bar{H}(\bar{x}) \qquad (A.6)$$

By substituting equation (A.6) into (A.2)

$$\bar{\nabla}\times\bar{E}(\bar{x}) = -j\omega\bar{\nabla}\times\bar{A}(\bar{x})$$

$$\text{or } \bar{\nabla}\times(\bar{E}(\bar{x}) + j\omega\bar{A}(\bar{x})) = 0 \qquad \text{(A.7)}$$

From equation (A.7), it is evident that $\bar{E} + j\omega\bar{A}$ equals to the gradient of a scalar. This leads to the definition of scalar potential V as

$$\bar{\nabla}V(\bar{x}) = -\bar{E}(\bar{x}) + j\omega\bar{A}(\bar{x}) \qquad \text{(A.8)}$$

From equation (A.1) and (A.6)

$$\bar{\nabla}\times\bar{\nabla}\times\bar{A}(\bar{x}) = j\omega\mu\varepsilon\bar{E}(\bar{x}) + \mu\bar{J}(\bar{x}) \qquad \text{(A.9)}$$

Applications of vector identity $\bar{\nabla}\times\bar{\nabla}\times\bar{A}(\bar{x}) = \bar{\nabla}\bar{\nabla}\cdot\bar{A}(\bar{x}) - \bar{\nabla}^2\bar{A}(\bar{x})$, and equation (A.8) to (A.9) yields.

$$\bar{\nabla}\bar{\nabla}\cdot\bar{A}(\bar{x}) - \bar{\nabla}^2\bar{A}(\bar{x}) = -j\omega\mu\varepsilon\bar{\nabla}V(\bar{x}) + \omega^2\mu\varepsilon\bar{A}(\bar{x}) + \mu\bar{J}(\bar{x}) \qquad \text{(A.10)}$$

or

$$\bar{\nabla}^2\bar{A}(\bar{x}) + k^2\bar{A}(\bar{x}) = \bar{\nabla}[\bar{\nabla}\cdot\bar{A}(\bar{x}) + j\omega\mu\varepsilon V(\bar{x})] - \mu\bar{J}(\bar{x}) \qquad \text{(A.11)}$$

where $k\ (=\omega\sqrt{\mu\varepsilon})$ is wave number.

Using Lorentz gauge condition,

$$\bar{\nabla}\cdot\bar{A}(\bar{x}) + j\omega\mu\varepsilon V(\bar{x}) = 0$$

equation (A.11) reduces to

$$\bar{\nabla}^2\bar{A}(\bar{x}) + k^2\bar{A}(\bar{x}) = -\mu\bar{J}(\bar{x}) \qquad \text{(A.12)}$$

which is equation (2.1) and is known as Helmholtz equation.

A.2 Direct Derivation of Equation (2.10b)

As pointed out in Section 2, the equation (2.10b) can be derived directly from Maxwell's equations and the equation of continuity without using the concept of vector potential.

By taking the curl of equation (A.2)

$$\bar{\nabla}\times\bar{\nabla}\times\bar{E}(\bar{x}) = -j\omega\mu\bar{\nabla}\times\bar{H}(\bar{x}) \tag{A.13}$$

Again using the vector identity of equation (2.7) and equation (A.1), (A.13) becomes

$$\bar{\nabla}\bar{\nabla}\cdot\bar{E}(\bar{x}) - \bar{\nabla}^2\bar{E}(\bar{x}) = -j\omega\mu(j\omega\varepsilon\bar{E}(\bar{x}) + \bar{J}(\bar{x}))$$

$$\text{or} \quad \bar{\nabla}^2\bar{E}(\bar{x}) + k^2\bar{E}(\bar{x}) = \bar{\nabla}\bar{\nabla}\cdot\bar{E}(\bar{x}) + j\omega\mu\bar{J}(\bar{x}) \tag{A.14}$$

By applying equation (A.3) to (A.14)

$$\bar{\nabla}^2\bar{E}(\bar{x}) + k^2\bar{E}(\bar{x}) = \frac{1}{\varepsilon}\bar{\nabla}\rho_c + j\omega\mu\bar{J}(\bar{x}) \tag{A.15}$$

Now the application of continuity equation (A.5) to (A.15) yields

$$\bar{\nabla}^2\bar{E}(\bar{x}) + k^2\bar{E}(\bar{x}) = -\frac{1}{j\omega\varepsilon}\bar{\nabla}\bar{\nabla}\cdot\bar{J}(\bar{x}) + j\omega\mu\bar{J}(\bar{x})$$

$$= -\frac{1}{j\omega\varepsilon}[\bar{\nabla}\bar{\nabla}\cdot + k^2]\bar{J}(\bar{x})$$

$$\text{or} \quad \bar{\nabla}^2\bar{E}(\bar{x}) + k^2\bar{E}(\bar{x}) = -\frac{1}{j\omega\varepsilon}T(\bar{J}(\bar{x})) \tag{A.16}$$

where T is linear differential operator as defined in Section 2 as $(\bar{\nabla}\bar{\nabla}\cdot + k^2)$.

The solution of equation (A.16), by analogy with equations (2.1) and (2.5), is given by

$$\bar{E}(\bar{x}) = \frac{1}{j\omega\varepsilon}[T(\bar{J}(\bar{x})) * K(\bar{x})] \qquad (A.17)$$

or $$\bar{E}(\bar{x}) = T(J(\bar{x})) * K_o(\bar{x}) \qquad (A.18)$$

where $K(\bar{x})$ and $K_o(\bar{x})$ are defined by equations (2.2) and (2.11) respectively.

It can be seen that equation (A.18) is the same as tion (2.10b) and due to commutation of convolution and differentiation, equation (2.10a) follows from (A.18).

APPENDIX B

B.1 The Axial Electrical Field E_z

The axial electrical field $E_z(\bar{x})$ may be obtained from either equations (2.10a) or (2.10b). From (2.10b)

$$E_z(\bar{x}) = [T[\bar{J}(\bar{x})]]_z * K_o(\bar{x}) \qquad (B.1)$$

where $K_o(\bar{x})$ is given by equation (2.11) and

$$[T[\bar{J}(\bar{x})]]_z = \frac{\partial^2 J_x}{\partial z \partial x} + \frac{\partial^2 J_y}{\partial z \partial y} + \frac{\partial^2 J_z}{\partial z^2} + k^2 J_z \qquad (B.2)$$

For cylindrical coordinate (z,ρ,ϕ) equation (B.2) can be written as

$$[T[\bar{J}(z,\rho,\phi)]]_z = \frac{1}{\rho}\frac{\partial^2(\rho J_\rho)}{\partial z \partial \rho} + \frac{\partial^2 J_\phi}{\rho \partial z \partial \phi} + \frac{\partial^2 J_z}{\partial z^2} + k^2 J_z \qquad (B.3)$$

For the basic linear element of equation (3.1), equation (B.3) reduces to

$$[T[\bar{J}(z,\rho)]]_z = [\frac{d^2}{dz^2} + k^2]J_z$$

$$= [\frac{d^2}{dz^2} + k^2]\frac{I_z(z)}{2\pi a}\delta(\rho-a)$$

$$= T_z[I_z(z)]\frac{\delta(\rho-a)}{2\pi a}, \quad |z| \leq L \qquad (B.4)$$

where $T_z = \left(\frac{d^2}{dz^2} + k^2\right)$ (B.5)

Hence equation (B.1) becomes

$$E_z(z,\rho,\phi) = T_z[I_z(z)] \frac{\delta(\rho-a)}{2\pi a} * K_o(\bar{x}) \quad \text{(B.6)}$$

Let us consider equation (B.6).

Now

$$K_o(\bar{x}) = \frac{\exp[-jkr(\bar{x})]}{j4\pi\omega\epsilon r(\bar{x})} \quad \text{(B.7)}$$

with $r(\bar{x}) = (x^2 + y^2 + z^2)^{\frac{1}{2}}$ (B.8)

therefore

$$r(\bar{x}-\bar{x}') = \{(x-x')^2 + (y-y')^2 + (z-z')^2\}^{\frac{1}{2}}$$

$$= \{(z-z')^2 + \rho^2 + \rho'^2 - 2\rho\rho'\cos(\phi-\phi')\}^{\frac{1}{2}} \quad \text{(B.9)}$$

Now by carrying out the integration in equation (B.6) with respect to ρ' and ϕ' this yields

$$E_z(z,\rho,\phi) = T_z[I_z] * K_z(z,\rho,\phi) \quad \text{(B.10)}$$

where the convolution is restricted to z and,

$$K_z(z,\rho,\phi) = \frac{1}{2\pi}\int_o^{2\pi} K_o(z,\rho,\phi-\phi')d\phi' \quad \text{(B.11)}$$

where K_o is given by equation (B.7) with

$$r(z,\rho,\phi) = \{z^2 + \rho^2 + a^2 - 2\rho a\cos\phi\}^{\frac{1}{2}} \quad \text{(B.12)}$$

It may be seen that equation (B.11) is independent of ϕ and so equation (B.6) can be written as

$$E_z(z,\rho) = T_z[I_z(z)] * K_z(z,\rho) \qquad (B.13)$$

where

$$K_z(z,\rho) = \frac{1}{2\pi}\int_0^{2\pi} K_o(z,\rho,\phi)\,d\phi \qquad (B.14)$$

Equation (B.13) is the same as (3.2).

B.2 The Radial Electrical Field E_ρ

The radial electrical field may also be obtained from either equations (2.10a) or (2.10b). From (2.10a)

$$E_\rho(\bar{x}) = [T[\bar{J}(\bar{x}) * K_o(\bar{x})]]_\rho \qquad (B.15)$$

where $K_o(\bar{x})$ is given by equation (B.7) and

$$[T[\bar{J}(\bar{x}) * K_o(\bar{x})]]_\rho = \frac{\partial}{\partial\rho}\left[\frac{\partial(\rho J_\rho * K_o(\bar{x}))}{\rho\,\partial\rho}\right] + \frac{\partial}{\partial\rho}\left[\frac{\partial(J_\phi * K_o(\bar{x}))}{\rho\,\partial\phi}\right] + \frac{\partial^2(J_z * K_o(\bar{x}))}{\partial\rho\,\partial z} + k^2 J_\rho \qquad (B.16)$$

For the basic linear element of equation (3.1) and through equation (B.16), equation (B.15) reduces to

$$E_\rho(\bar{x}) = \frac{\partial^2}{\partial\rho\,\partial z}[J_z * K_o(\bar{x})]$$

$$= \frac{\partial^2}{\partial\rho\,\partial z}\left[I_z(z)\,\frac{\delta(\rho-a)}{2\pi a} * K_o(\bar{x})\right] \qquad (B.17)$$

Carrying out the convolution with respect to x and y, as shown similarly in Appendix (B.1), equation (B.17) reduces to

$$E_\rho(z,\rho) = \frac{\partial^2}{\partial\rho\,\partial z}\,[I_z(z) * K_z(z,\rho)] \qquad (B.18)$$

where $K_z(z,\rho)$ is given by equations (3.6) or (B.14) and the convolution is restricted to z only. Since in (B.18) convolution and differentiations commute, it can be rewritten as

$$E_\rho(z,\rho) = I_z(z) * \frac{\partial^2}{\partial\rho\,\partial z}\,K_z(z,\rho) \qquad (B.19)$$

Now

$$\frac{\partial^2}{\partial\rho\,\partial z}\,[K_z(z,\rho)] = -\,T_z[K_\rho(z,\rho)] \qquad (B.20)$$

where T_z is defined by equations (3.5) or (B.5) and,

$$K_\rho(z,\rho) = \frac{1}{2\pi}\int_0^{2\pi} \frac{z(\rho - a\cos\phi)}{\rho^2+a^2-2\rho a\cos\phi}\,K_o(z,\rho,\phi)\,d\phi \qquad (B.21)$$

where K_o is given by equations (B.7) through (B.12).

Therefore,

$$E_\rho(z,\rho) = -I_z(z) * (-T_z[K_\rho(z,\rho)])$$

$$= -\,T_z[I_z(z)] * K_\rho(z,\rho) \qquad (B.22)$$

which is equation (3.3).

B. 3 The Angular Electrical Field E_ϕ

The angular electrical field E_ϕ can be obtained from either equations (2.10a) or (2.10b). From (2.10b)

$$E_\phi(\bar{x}) = [T[J(\bar{x})]]_\phi * K_o(\bar{x}) \tag{B.23}$$

where $K_o(\bar{x})$ is given by equation (B.7) and

$$[T[\bar{J}(\bar{x})]]_\phi = \frac{1}{\rho}\frac{\partial}{\partial\phi}\left[\frac{\partial(\rho J_\rho)}{\rho\partial\rho}\right] + \frac{1}{\rho^2}\frac{\partial^2 J_\phi}{\partial\phi} + \frac{1}{\rho}\frac{\partial^2 J_z}{\partial\phi\partial z} + k^2 J_\phi \tag{B.24}$$

For the basic linear element of equation (3.1) equation (B.24) reduces to

$$\begin{aligned}[T[\bar{J}(z,\rho)]]_\phi &= \frac{1}{\rho}\frac{\partial^2 J_z}{\partial\phi\partial z} \\ &= \frac{1}{\rho}\frac{\partial^2}{\partial\phi\partial z}\left[\frac{I_z(z)\,\delta(\rho-a)}{2\pi a}\right] \\ &= 0\end{aligned} \tag{B.25}$$

Using equation (B.25) in (B.23) it reduces to

$$E_\phi(\bar{x}) = 0 \tag{B.26}$$

which is equation (3.4)

B.4 Integrations of Composite Kernel K_{zac} and Green's Function $G(z/z')$

For a basic linear element for calculating the scattered field, the approximate composite kernel K_{zac} can be written from equation (3.19) through equations (3.23) and

(3.24) as

$$K_{zac}(z/z'/0) = K_{za}(z-z',0) - K_{za}(z+L,0)\frac{\sin[k(L-z')]}{\sin(2kL)}$$

$$- K_{za}(z-L,0)\frac{\sin[k(L+z')]}{\sin(2kL)} \qquad (B.27)$$

where the approximate kernel $K_{za}(z,0)$ is given by (3.26).

Using point matching in conjunction with pulse functions of equation (3.46), the equation for the scattered field is given as

$$\sum_{j=1}^{n} g_j \int_{q_1}^{q_2} K_{zac}(z_i/z'/0)dz' = - E_z^i(z_i,0) \qquad (B.28)$$

$$\text{for } i = 1,2, \ldots, n$$

where q_1 and q_2 are the lower and upper limits of $\Delta z_j'$ for j^{th} segment of equation (3.46) for pulse functions. From equation (B.27) the integration of K_{zac} may be given as

$$\int_{q_1}^{q_2} K_{zac}(z_i/z'/0) = \int_{q_1}^{q_2} K_{za}(z_i-z',0)dz' - K_{za}(z_i+L,0)$$

$$\int_{q_1}^{q_2} \frac{\sin[k(L-z')]}{\sin(2kL)}dz' - K_{za}(z_i-L,0)$$

$$\int_{q_1}^{q_2} \frac{\sin[k(L+z')]}{\sin(2kL)}dz' \qquad (B.29)$$

or

$$\int_{q_1}^{q_2} K_{zac}(z_i/z'/0) \left\{ = \int_{q_1}^{q_2} K_{za}(z_i-z',0)dz' + [h_1 K_{za}(z_i+L,0) \right.$$

$$\left. - h_2 K_{za}(z_i-L,0)] \right. \tag{B.30}$$

where

$$h_1 = \{\cos[k(L-q_1)] - \cos[k(L-q_2)]\}/k \sin(2kL)$$

$$h_2 = \{\cos[k(L+q_1)] - \cos[k(L+q_2)]\}/k \sin(2kL) \tag{B.31}$$

Similarly the equation for current distributions may be given from (3.35) as

$$I_z(z) = \sum_{j=1}^{n} q_j \int_{q_1}^{q_2} G(z/z')dz' \tag{B.32}$$

where Green's function $G(z/z')$ is given by (3.16). The closed form of integration of $G(z/z')$ may be given as

$$\int_{q_1}^{q_2} G(z/z')dz' =$$

$$\begin{cases} h_1 \sin[k(L+z)]/k, & z \leq q_1 \\ \frac{1}{k^2} - \{\sin[k(L-z)]\cos[k(L+q_1)] + \\ \sin[k(L+z)]\cos[k(L-q_2)]\}/ \\ \{k^2 \sin(2kL)\}, & q_1 \leq z \leq q_2 \\ -h_2 \sin[k(L-z)]/k, & z \geq q_2 \end{cases} \tag{B.33}$$

APPENDIX C

C.1 Cancellation of Higher Order Fields in Multi-Element Systems

If at any point in space n elements of equal radii a are joined together then the higher order fields, i.e., terms with derivatives in equations (4.1) and (4.2) using approximate kernels, cancel when Kirchoff's current law is applied at the joint. Consider n such elements 1, 2, . . . n of respective half lengths $L_1, L_2, \ldots L_n$ axially joined together in space at a point A as shown in Figure C.1. Let there be an observation point B at a distance t from A in space where the resultant field from all n elements has to be evaluated. The angle between element 1 and AB is θ_1, between element 2 and AB is θ_2 and so on for all the elements. From equations (4.1) and (4.2) the radiated axial and radial fields from element 1 can be written using approximate kernels as

$$E_{z_1}(z_1,\rho_1) = \int_{-L_1}^{L_1} E_{o1}(z_1') K_{z_1 ac}(z_1/z_1'/\rho_1)\,dz_1'$$

$$+ I_{z_1}(-L_1)K'_{z_1 a}(z_1+L_1,\rho_1) - I_{z_1}(L_1)K'_{z_1 a}(z_1-L_1,\rho_1)$$

$$+ b_1 K_{z_1 a}(z_1+L_1,\rho_1) - c_1 K_{z_1 a}(z_1-L_1,\rho_1) \qquad (C.1)$$

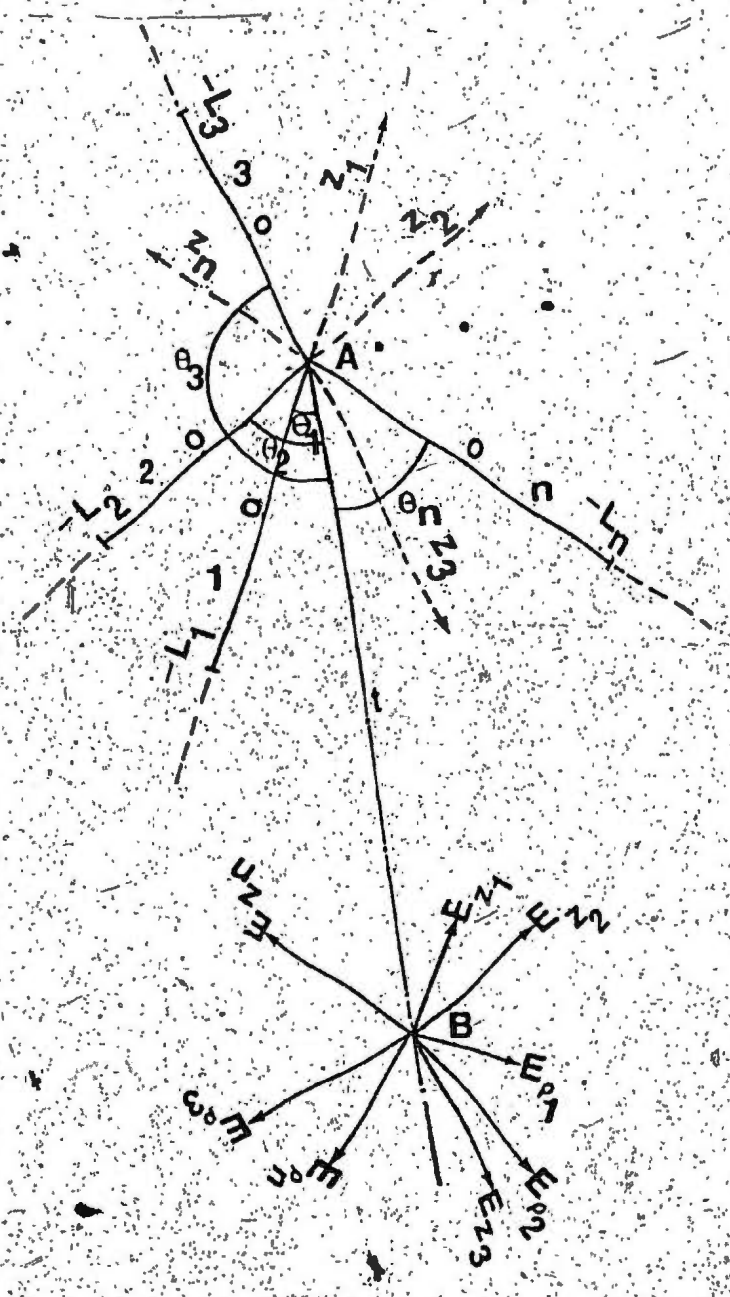

Figure C.1. Geometry of n elements of equal radii a axially joined together at their one end in space at A, B any observation point.

and

$$E_{\rho_1}(z_1,\rho_1) = -\left[\int_{-L_1}^{L_1} E_{o1}(z_1')K_{\rho_1 ac}(z_1/z_1'/\rho_1)\,dz_1'\right.$$

$$+ I_{z_1}(-L_1)K'_{\rho_1 a}(z_1+L_1,\rho_1) - I_{z_1}(L_1)K'_{\rho_1 a}(z_1-L_1,\rho_1)$$

$$\left. + b_1 K_{\rho_1 a}(z_1+L_1,\rho_1) - c_1 K_{\rho_1 a}(z_1-L_1,\rho_1)\right], \qquad (C.2)$$

where all the quantities have been defined earlier. The primes denote the differentiation with respect to z_1. Applying simple calculus to equation (C.2) it can be rewritten as

$$E_{\rho_1}(z_1,\rho_1) = -\left[\int_{-L_1}^{L_1} E_{o1}(z_1')K_{\rho_1 ac}(z_1/z_1'/\rho_1)\,dz_1'\right.$$

$$- I_{z_1}(-L_1)\frac{d}{d\rho_1}K_{z_1 a}(z_1+L_1,\rho_1) + I_{z_1}(L_1)\frac{d}{d\rho_1}$$

$$K_{z_1 a}(z_1-L_1,\rho_1) + d_1 K_{\rho_1 a}(z_1+L_1,\rho_1)$$

$$\left. - e_1 K_{\rho_1 a}(z_1-L_1,\rho_1)\right], \qquad (C.3)$$

where d_1 and e_1 are defined by equations (4.13) and (4.14) respectively.

From equation (4.4) for $K_{z_1 a}$ its derivatives with respect to z_1 and ρ_1 can be given as

$$\frac{d}{dz_1}K_{z_1 a}(z_1,\rho_1) = -z_1\frac{[1+jkr(z_1,\rho_1)]}{[r(z_1,\rho_1)]^2}K_{z_1 a}(z_1,\rho_1) \qquad (C.4)$$

$$\frac{d}{d\rho_1} K_{z_1 a}(z_1, \rho_1) = - \rho_1 \frac{[1+jkr(z_1, \rho_1)]}{[r(z_1, \rho_1)]^2} K_{z_1 a}(z_1, \rho_1) \qquad (C.5)$$

$$\text{where } r(z_1, \rho_1) = (z_1^2 + \rho_1^2 + a^2)^{\frac{1}{2}} \qquad (C.6)$$

Now only the higher order fields, i.e., the terms with derivatives in equations (C.1) and (C.3) will be considered for all n elements. It may be noted these fields arise when end currents are not zero. For free ends no such fields are present since end currents are zero.

Element 1:

From Figure C.1 the coordinates (z_1, ρ_1) of B with respect to axis z_1 of element 1 is

$$z_1 = L_1 - t \cos\theta_1$$

$$\rho_1 = t \sin\theta_1$$

The axial and radial components of higher order field from this element at B are then

$$E_{z_1} = - I_{z_1}(L_1) \frac{d}{dz_1} K_{z_1 a}(-t \cos\theta_1, t \sin\theta_1)$$

$$= - I_{z_1}(L_1) G \cos\theta_1 \qquad (C.7)$$

$$E_{\rho_1} = - I_{z_1}(L_1) \frac{d}{d\rho_1} K_{z_1 a}(-t \cos\theta_1, t \sin\theta_1)$$

$$= I_{z_1}(L_1) G \sin\theta_1 \qquad (C.8)$$

where,

$$G = t \frac{1+jk(t^2+a^2)^{\frac{1}{2}}}{j4\pi\omega\varepsilon(t^2+a^2)^{3/2}} \exp[-jk(t^2+a^2)^{\frac{1}{2}}] \qquad (C.9)$$

Application of vector addition to these two field components in the coordinate systems used yields that the resultant lies in the direction of AB with magnitude

$$|\bar{E}_1| = G\, I_{z_1}(L_1) \qquad (C.10)$$

Element 2:

Again from Figure C.1 the coordinates (z_2, ρ_2) of B with respect to axis z_2 of element 2 is

$$z_2 = L_2 - t\cos\theta_2$$

$$\rho_2 = t\sin\theta_2$$

The axial and radial components of higher order fields from this element at B are then

$$E_{z_2} = -I_{z_2}(L_2)\, G\cos\theta_2 \qquad (C.11)$$

$$E_{\rho_2} = I_{z_2}(L_2)\, G\sin\theta_2 \qquad (C.12)$$

where G is given by (C.9).

The resultant of the above two fields again lies in the direction of AB with magnitude

$$|\bar{E}_2| = G\, I_{z_2}(L_2) \qquad (C.13)$$

Similarly, this can be extended for n such elements. For n^{th} element the above field at B due to it may be given as

$$E_{z_n} = - I_{z_n}(L_n)\, G \cos\theta_n \qquad (C.14)$$

$$E_{\rho_n} = I_{z_n}(L_n)\, G \sin\theta_n \qquad (C.15)$$

The resultant again lies in the direction of AB with the magnitude

$$|\bar{E}_n| = I_{z_n}(L_n)\, G \qquad (C.16)$$

Thus it may be seen that for the given configuration of n elements in Figure C.1 the resultant of axial and radial higher order fields for each element lies in the direction of AB with different magnitudes. The magnitude of net resultant is then just the scalar addition of magnitudes of all the resultants, i.e.,

$$|\bar{E}| = G\, I_{z_1}(L_1) + G\, I_{z_2}(L_2) + \ldots + G\, I_{z_n}(L_n) \qquad (C.17)$$

Kirchoff's current law at junction A gives

$$I_{z_1}(L_1) + I_{z_2}(L_2) + \ldots + I_{z_n}(L_n) = 0 \qquad (C.18)$$

Application of (C.18) to (C.17) yields

$$|\bar{E}| = 0 \qquad (C.19)$$

or $$\bar{E} = 0 \qquad (C.20)$$

Hence, equations (4.11) and (4.12) follow from (C.20) through equations (C.1) and (C.3). If any other configuration for a joint is given, it can be easily transformed into this above configuration and cancellation of higher order terms proved.

C.2 Coupled Integral Equations for a Joined Two Element Structure

Let the two elements 1 and 2 of equal radii a and respective half lengths L_1 and L_2 be axially joined together at their ends (L_1, L_2) as shown in Figure 4.1(ii). For simplicity only their axes are shown in figure. The angle between their axes is θ. Since their other ends $(-L_1, -L_2)$ are free, $I_{z_1}(-L_1)$ and $I_{z_2}(-L_2)$ vanish. For this case equations (4.7) and (4.8) can be expanded with the help of equations (4.11) and (4.12) and Figure 4.1(ii) as,

$$\int_{-L_1}^{L_1} E_{o1}(z_1') K_{z_1 ac}(z_1/z_1'/0)dz_1' + \int_{-L_2}^{L_2} E_{o2}(z_2')\{\cos\theta K_{z_2 ac}(z_2/z_2'/\rho_2) + \sin\theta K_{\rho_2 ac}(z_2/z_2'/\rho_2)\}dz_2' - I_{z_1}(L_1)\{u_1 K_{z_1 a}(z_1-L_1,0) - v_1 K_{z_1 a}(z_1+L_1,0)\} - I_{z_2}(L_2)[\cos\theta\{u_2 K_{z_2 a}(z_2-L_2,\rho_2) - v_2 K_{z_2 a}(z_2+L_2,\rho_2)\} + \sin\theta\{u_2 K_{\rho_2 a}(z_2-L_2,\rho_2) - v_2 K_{\rho_2 a}(z_2+L_2,\rho_2) - \frac{jk}{z_2-L_2} r(z_2-L_2,\rho_2) K_{\rho_2 a}(z_2-L_2,\rho_2)\}] \quad (C.21)$$

$$= - E^i_{z_1}(z_1, 0)$$

and

$$\int_{-L_1}^{L_1} E_{o1}(z_1')\{\cos\theta K_{z_1 ac}(z_1/z_1'/\rho_1) + \sin\theta K_{\rho_1 ac}(z_1/z_1'/0)\}dz_1'$$

$$+ \int_{-L_2}^{L_2} E_{o2}(z_2') K_{z_2 ac}(z_2/z_2'/0)dz_2' - I_{z_1}(L_1)[\cos\theta\{u_1$$

$$K_{z_1 a}(z_1-L_1,\rho_1) - v_1 K_{z_1 a}(z_1+L_1,\rho_1)\} + \sin\theta\{u_1 K_{\rho_1 a}(z_1-L_1,\rho_1)$$

$$- v_1 K_{\rho_1 a}(z_1+L_1,\rho_1) - \frac{jk}{z_1+L_1} r(z_1-L_1,\rho_1) K_{\rho_1 a}(z_1-L_1,\rho_1)\}] - I_{z_2}(L_2)\{u_2$$

$$K_{z_2 a}(z_2-L_2,0) - v_2 K_{z_2 a}(z_2+L_2,0)\} = -E^i_{z_2}(z_2,0) \qquad \text{(C.22)}$$

where

$$u_1 = \frac{k\cos(2kL_1)}{\sin(2kL_1)} \qquad \text{(C.23)}$$

$$u_2 = \frac{k\cos(2kL_2)}{\sin(2kL_2)} \qquad \text{(C.24)}$$

$$v_1 = \frac{k}{\sin(2kL_1)} \qquad \text{(C.25)}$$

$$v_2 = \frac{k}{\sin(2kL_2)} \qquad \text{(C.26)}$$

$K_{z_1 ac}(z_1/z_1'/\rho_1)$, $K_{z_2 ac}(z_2/z_2'/\rho_2)$, $K_{\rho_1 ac}(z_1/z_1'/\rho_1)$, and

$K_{\rho_2 ac}(z_2/z_1'/\rho_2)$ are given from equations (3.19) and (3.20)

after replacing the actual kernels by their approximations as

$$K_{z_1 ac}(z_1/z_1'/\rho_1) = K_{z_1 a}(z_1-z_1',\rho_1) - \frac{\sin[k(L_1-z_1')]}{\sin(2kL_1)}$$

$$K_{z_1 a}(z_1+L_1,\rho_1) - \frac{\sin[k(L_1+z_1')]}{\sin(2kL_1)} K_{z_1 a}(z_1-L_1,\rho_1) \qquad (C.27)$$

$$K_{z_2 ac}(z_2/z_2'/\rho_2) = K_{z_2 a}(z_2-z_2',\rho_2) - \frac{\sin[k(L_2-z_2')]}{\sin(2kL_2)}$$

$$K_{z_2 a}(z_2+L_2,\rho_2) - \frac{\sin[k(L_2+z_2')]}{\sin(2kL_2)} K_{z_2 a}(z_2-L_2,\rho_2) \qquad (C.28)$$

$$K_{\rho_1 ac}(z_1/z_1'/\rho_1) = K_{\rho_1 a}(z_1-z_1',\rho_1) - \frac{\sin[k(L_1-z_1')]}{\sin(2kL_1)}$$

$$K_{\rho_1 a}(z_1+L_1,\rho_1) - \frac{\sin[k(L_1+z_1')]}{\sin(2kL_1)} K_{\rho_1 a}(z_1-L_1,\rho_1) \qquad (C.29)$$

$$K_{\rho_2 ac}(z_2/z_2'/\rho_2) = K_{\rho_2 a}(z_2-z_1',\rho_2) - \frac{\sin[k(L_2-z_2')]}{\sin(2kL_2)}$$

$$K_{\rho_2 a}(z_2+L_2,\rho_2) - \frac{\sin[k(L_2+z_2')]}{\sin(2kL_2)} K_{\rho_2 a}(z_2-L_2,\rho_2) \qquad (C.30)$$

where approximate kernels $K_{z_1 a}$ and $K_{\rho_1 a}$ are given by equations (4.4) and (4.6) respectively, and similarly $K_{z_2 a}$ and $K_{\rho_2 a}$ given.

r in general is defined by equation (4.15) as,

$$r(z,\rho) = (z^2+\rho^2+a^2)^{\frac{1}{2}} \qquad (C.31)$$

In equation (C.21), z_2 and ρ_2 are the coordinates of any observation point on z_1 with respect to the coordinate system $(\bar{x}_2)$ of element 2. These can be given from Figure 4.1(ii) as,

$$z_2 = L_2 - (L_1-z_1)\cos\theta \qquad (C.32)$$

$$\rho_2 = (L_1-z_1)\sin\theta \qquad (C.33)$$

Similarly in equation (C.22), z_1 and ρ_1 are the coordinates of any observation point on z_2' with respect to coordinate system $(\bar{x}_1)$ of element 1. These can be given as,

$$z_1 = L_1 - (L_2-z_2)\cos\theta \qquad (C.34)$$

$$\rho_1 = (L_2-z_2)\sin\theta \qquad (C.35)$$

Therefore, equations (C.32) and (C.33) should be applied to equation (C.21) for replacing z_2 and ρ_2. Similarly, equations (C.34) and (C.35) should be applied to equation (C.22) for replacing z_1 and ρ_1. z_1' and z_2' in equations (C.21) and (C.22) are only the integration variables. Thus for a given incident field $E^i_{z_1}$ and $E^i_{z_2}$ from some external source, equations (C.21) and (C.22) result in a form of a coupled integral equations for a case of two elements joined together with unknowns of $E_{o1}(z_1')$, $E_{o2}(z_2')$ and the end currents $I_{z_1}(L_1)$ and $I_{z_2}(L_2)$. A third equation is obtained by

applying Kirchoff's current law at the junction as

$$I_{z_1}(L_1) + I_{z_2}(L_2) = 0 \qquad (C.36)$$

C.3 Integration of Composite Kernel $K_{\rho ac}$

It is indicated in Section 4.2 that by using point matching technique in conjunction with pulse functions of equation (3.46) for solving the integral equations for a multi-element structure the integration involved for the radial electrical field (E_ρ) is limited to that of the composite kernel $K_{\rho ac}$ and is available in closed form. The closed form of this integration can be given as follows.

From equation (3.20) through equations (3.23) and (3.24) the approximate composite kernel $K_{\rho ac}$ may be given after replacing the actual kernel K_ρ by its approximation $K_{\rho a}$ as

$$K_{\rho ac}(z/z'/\rho) = K_{\rho a}(z-z',\rho) - K_{\rho a}(z+L,\rho)\frac{\sin[k(l-z')]}{\sin(2kL)}$$

$$- K_{\rho a}(z-L,\rho)\frac{\sin[k(L+z')]}{\sin(2kL)} \qquad (C.37)$$

where $K_{\rho a}(z,\rho)$ is the approximate kernel given by equation (4.6) as

$$K_{\rho a}(z,\rho) = \frac{z\rho}{\rho^2+a^2} K_{za}(z,\rho) \qquad (C.38)$$

where the approximate kernel K_{za} is given by equation (4.4)

as

$$K_{za}(z,\rho) = \frac{\exp[-jkr(z,\rho)]}{j4\pi\omega\varepsilon r(z,\rho)} \qquad (C.39)$$

with

$$r(z,\rho) = (z^2+\rho^2+a^2)^{\frac{1}{2}} \qquad (C.40)$$

Therefore, its integral over q_1 to q_2 where q_1 and q_2 are again the lower and upper limits of $\Delta z_j'$ for j^{th} segment of equation (3.46) for pulse functions, may be written as

$$\int_{q_1}^{q_2} K_{\rho ac}(z/z'/\rho)dz' = \int_{q_1}^{q_2} K_{\rho a}(z-z',\rho)dz' + [h_1 K_{\rho a}(z+L,\rho) - h_2 K_{\rho a}(z-L,\rho)] \qquad (C.41)$$

where h_1 and h_2 are defined by equation (B.31) as

$$h_1 = \{\cos[k(L-q_1)] - \cos[k(L-q_2)]\}/k \sin(2kL)$$
$$h_2 = \{\cos[k(L+q_1)] - \cos[k(L+q_2)]\}/k \sin(2kL) \qquad (C.42)$$

From equations (C.38) to (C.40) the integral on right hand side of equation (C.41) may be written as

$$\int_{q_1}^{q_2} K_{\rho a}(z-z',\rho)dz' = \int_{q_1}^{q_2} \frac{(z-z')\rho}{\rho^2+a^2} \frac{\exp[-jkr(z-z',\rho)]}{j4\pi\omega\varepsilon r(z-z',\rho)} dz' \qquad (C.43)$$

By simple substitution of

$$(z-z')^2 + \rho^2 + a^2 = D^2$$

for the integration, the right hand side of equation (C.43) may be evaluated as

$$= \frac{j\rho}{k(\rho^2+a^2)} [r(z-q_1,\rho)\, K_{za}(z-q_1,\rho) - r(z-q_2,\rho)\, K_{za}(z-q_2,\rho)] \qquad (C.44)$$

Application of equation (C.44) in (C.41) yields the integration of $K_{\rho ac}$ in closed form.


CENTRE FOR NFLD. STUDIES
JUL 18 1979
MEMORIAL UNIVERSITY
OF NEWFOUNDLAND